

Computed tomography analysis of the cranium of *Champsosaurus lindoei* and implications for the choristoderan neomorphic ossification

Thomas W. Dudgeon¹  Hillary C. Maddin,¹ David C. Evans^{2,3} and Jordan C. Mallon^{1,4}

¹Department of Earth Sciences, Carleton University, Ottawa, Canada

²Vertebrate Palaeontology, Royal Ontario Museum, Toronto, Canada

³Department of Ecology and Evolutionary Biology, University of Toronto, Toronto, Canada

⁴Beaty Centre for Species Discovery and Palaeobiology Section, Canadian Museum of Nature, Ottawa, Canada

Abstract

Choristoderes are extinct neodiapsid reptiles that are well known for their unusual cranial anatomy, possessing an elongated snout and expanded temporal arches. Although choristodere skulls are well described externally, their internal anatomy remains unknown. An internal description was needed to shed light on peculiarities of the choristodere skull, such as paired gaps on the ventral surface of the skull that may pertain to the fenestra ovalis, and a putative neomorphic ossification in the lateral wall of the braincase. Our goals were: (i) to describe the cranial elements of *Champsosaurus lindoei* in three dimensions; (ii) to describe paired gaps on the ventral surface of the skull to determine if these are indeed the fenestrae ovals; (iii) to illustrate the morphology of the putative neomorphic bone; and (iv) to consider the possible developmental and functional origins of the neomorph. We examined the cranial anatomy of the choristodere *Champsosaurus lindoei* (CMN 8920) using high-resolution micro-computed tomography scanning. We found that the paired gaps on the ventral surface of the skull do pertain to the fenestrae ovals, an unusual arrangement that may be convergent with some plesiosaurs, some aistopods, and some urodeles. The implications of this morphology in *Champsosaurus* are unknown and will be the subject of future work. We found that the neomorphic bone is a distinct ossification, but is not part of the wall of the brain cavity or the auditory capsule. Variation in the developmental pathways of cranial bones in living amniotes was surveyed to determine how the neomorphic bone may have developed. We found that the chondrocranium and splanchnocranium show little to no variation across amniotes, and the neomorphic bone is therefore most likely to have developed from the dermatocranium; however, the stapes is a pre-existing cranial element that is undescribed in choristoderes and may be homologous with the neomorphic bone. If the neomorphic bone is not homologous with the stapes, the neomorph likely developed from the dermatocranium through incomplete fusion of ossification centres from a pre-existing bone, most likely the parietal. Based on the apparent morphology of the neomorph in *Coeruleodraco*, the neomorph was probably too small to play a significant structural role in the skull of early choristoderes and it may have arisen through non-adaptive means. In neochoristoderes, such as *Champsosaurus*, the neomorph was likely recruited to support the expanded temporal arches.

Key words: choristodera; skull anatomy; computed tomography; development; evolution.

Introduction

Choristoderes were small to medium-sized (30 cm–3 m long) neodiapsid reptiles that lived from the Middle Jurassic

(Bathonian) to the Miocene (Eggenburgian) of Laurasia (Evans & Klembara, 2005; Matsumoto & Evans, 2010). These animals are known for their unusual cranial morphology, characterized by an elongated preorbital region and posteriorly expanded temporal arches (Gao & Fox, 1998). *Champsosaurus* exhibits the most extreme condition of these features, where the snout has become particularly elongated and slender, comprising half the length of the skull. The temporal arches are also dramatically expanded posterolaterally, giving the skull a cordiform dorsal profile. Other unusual features of the skull of *Champsosaurus*

Correspondence

Thomas W. Dudgeon, Department of Earth Sciences, Herzberg Laboratories, Carleton University, 1125 Colonel By Drive, Ottawa, Ontario K1S 5B6, Canada. E: thomasdudgeon@cmail.carleton.ca

Accepted for publication 18 November 2019

Article published online 6 January 2020

include the presence of paired gaps on the ventral surface of the skull that border the parasphenoid laterally. These gaps were first identified by Russell (1956) as the external auditory meatuses, but have been subsequently interpreted as unossified gaps in the otic capsule that may have enclosed the stapes (Fox, 1968). These gaps have received no attention since their descriptions by Russell (1956) and Fox (1968), and the auditory system is undescribed among Choristodera.

Another peculiarity of the choristodere skull is the putative presence of a neomorphic bone in the lateral wall of the braincase. This bone was first identified by Fox (1968) as a small triangular element, having previously been identified as part of the squamosal (Brown, 1905) or prootic (Fox, 1968). Erickson (1972) later suggested that there was no evidence for the neomorphic bone in *Champsosaurus gigas*, and that this element was simply a misidentified extension of the parietal. More recent interpretations (Gao & Fox, 1998) have again suggested that the neomorph is indeed a distinct, elongate element, extending posteriorly to the pterygoquadrate foramen. Despite the previous uncertainty in the literature, subsequent descriptions of choristoderes follow the conclusions of Gao & Fox (1998) and refer to the neomorphic bone as a distinct ossification (e.g. Gao & Fox, 2005; Matsumoto et al. 2007; Gao & Ksepka, 2008; Matsumoto et al. 2019), but the neomorphic bone has yet to be properly described. Skepticism regarding its presence in the braincase region is well justified, as the morphology of the neomorph has been previously debated, and the braincase is considered to have remained relatively conserved throughout tetrapod evolution (Cardini & Elton, 2008; Goswami & Polly, 2010; Knoll et al. 2012; Maddin et al. 2012).

Fox (1968) stated that the neomorphic bone does not contact the endocranial cavity, but the relationship of this element to the brain cavity, endosseous labyrinth, and cranial nerve tracts has not been re-evaluated following its description as a larger element by Gao & Fox (1998). As such, the neomorphic bone requires an exhaustive three-dimensional (3D) description to determine its validity, and its relationship to the other cranial elements and endocranial structures.

The objectives of the present paper are fourfold. Using high-resolution micro-computed tomography, we aimed to: (i) describe the cranial elements of a well-preserved specimen of *Champsosaurus lindoei* (CMN 8920) in three dimensions; (ii) provide a description of the paired gaps reported on the ventral surface of the skull and investigate the hypothesis that these relate to the fenestrae oiales; (iii) illustrate the morphology of the putative neomorphic bone and discuss how it relates to other cranial elements and the internal structures of the skull (e.g. brain cavity, and endosseous labyrinth, cranial nerves); and (iv) consider the possible developmental and functional origins of the neomorph.

Definitions

The putative choristodere neomorphic bone has often been described as a component of the braincase (e.g. Fox, 1968; Brinkman & Dong, 1993; Gao & Fox, 2005; James, 2010), but in order to determine whether the putative neomorph is indeed a braincase element, the definition of a braincase bone needs to be established. There are three recurring definitions of braincase bones in the literature: (1) only bones of the chondrocranium (Romer, 1956); (2) all bones of the chondrocranium plus the dermatocranial parasphenoid (Romer & Parsons, 1977; Atkins & Franz-Odenaal, 2016); and (3) all bones that enclose the brain cavity (Specht et al. 2007). The reason for the inclusion of the dermatocranial parasphenoid (definition 2) is well justified, as most lineages of amniotes fuse the parasphenoid with the basisphenoid (Atkins & Franz-Odenaal, 2016), and the parasphenoid plays a role in supporting the brain ventrally. The third definition is common in human and mammalian anatomy more generally (Hopson & Rougier, 1993; Specht et al. 2007), as the chondrocranial elements play a significantly smaller role in the mammalian cranium than they do in other lineages (Romer & Parsons, 1977). The issue with the third definition is that it includes several bones of either dermatocranial origin, or of mixed dermatocranial and chondrocranial origin, such as the mammalian temporal bone and sphenoid, respectively, making broad comparisons across lineages difficult (Porto et al. 2009).

The braincase is therefore defined in the present study using the second definition, which includes all bones of the chondrocranium, plus the parasphenoid. This definition is often used when discussing the braincase of reptiles (Romer, 1956; Romer & Parsons, 1977) and is therefore effective for comparisons across many lineages. As such, if the neomorphic bone is found to be a distinct ossification, it will only be considered here as a braincase bone if it could have ossified from the chondrocranium, or is tightly integrated or fused with other chondrocranial bones.

Institutional abbreviations

CMN, Canadian Museum of Nature, Ottawa, Ontario; IVPP, Institute of Vertebrate Paleontology and Paleoanthropology, Beijing, China; ROM, Royal Ontario Museum, Toronto, Ontario; SMM, Science Museum of Minnesota, St. Paul, Minnesota; TMP, Tyrrell Museum of Palaeontology; UALVP, Laboratory for Vertebrate Palaeontology, University of Alberta, Edmonton, Alberta; UTCT, University of Texas High-Resolution X-ray Computed Tomography Facility, Austin, Texas.

Anatomical abbreviations

Bone abbreviations in brackets indicate suture surfaces.

ac, passage for the anterior semicircular canal; art, articular surface for the jaws; bo, basioccipital; bs, basisphenoid;

bt, basal tubera; ca, impression of the internal carotid artery; cc, canal for the crus communis; ch, choana; CN I, passage for CN I; CN IX, exit for CN IX; CN V, opening for CN V; CN V_{2f}, foramen for CN V₂; CNV_{2n}, passage for CN V₂ and nasolacrimal duct; CN VI, canal for CN VI; mf, metotic foramen (canal for CN X and CN XI); CN XII, canal for CN XII; cp, clinoid process; d, midline depression; dc, dorsal concavity; dcp, dorsal concavity for pineal body; den, dentine; dr, dorsal ridge; dv, foramina for diploic veins; ect, ectopterygoid; en, enamel; ex, exoccipital; flan, flange for articulation with the first cervical vertebra; fm, foramen magnum; fr, frontal; fo, fenestra ovalis; gv, groove; hvnt, lateral head vein trough; hvnw, wall of lateral head vein; inc, incisive foramen; int, internarial; ita, inferior temporal arch; itf, infratemporal fenestra; itfw, wall of the infratemporal fenestra; ju, jugal; k, dorsal keel; lac, lacrimal; lat frk, lateral fork; lc, passage for the lateral semicircular canal; lshf, lacrimal shelf; max, maxilla; max alv, maxillary alveoli; med frk, medial fork; mpr, median pharyngeal recess; na, nasal; no, narial opening; ne, neomorph; npt, nasopalatal trough; nv, nasal vestibule; oc, occipital condyle; ocf, olfactory chamber floor; olf, dorsal impression of olfactory stalk; och, olfactory chamber; op; opisthotic; orb, orbit; orn, ornamentation; otc, otic capsule; pa, parietal; pal, palatine; pal alv, palatine alveoli; pc, passage for the posterior semicircular canal; pit, pituitary fossa; plc, plicidentine infolding; pm, premaxilla; pm alv, premaxillary alveoli; pof, postfrontal; pop, paroccipital process; por, postorbital; pr, prootic; prf, prefrontal; ps, parasphenoid; pt, pterygoid; pta, post-temporal arch; ptf, pterygoid flange; ptf, post-temporal fenestra; ptq, pterygoquadrate foramen; ptv, interpterygoid vacuity; pt alv, pterygoid alveoli; pul, pulp cavity; q, quadrate; qj, quadratojugal; qr, quadrate ramus; rid, ridges; sf, suborbital fenestra; sfw, wall of suborbital fenestra; shf, dorsal shelf extending ventral to the parietal; so, supraoccipital; sof, subolfactory flange; sq, squamosal; sta, superior temporal arch; stf, supratemporal fenestra; stfw, wall of the supratemporal fenestra; t, teeth; tf, temporal fossa; U, U-shaped groove; vfm, ventral rim of the foramen magnum; vo, vomer; vom alv, vomerine alveoli; vpn, ventral projection of the nasal; vpq, ventral projection of the quadrate; vs, vomerine septum; (i-max), intermaxillary contact.

Materials and methods

CMN 8920 was collected by H. L. Shearman on July 13, 1953 from the Dinosaur Park Formation on the east branch of Sand Creek, Alberta (NAD83; 12U 460541.290, 5619553.359). The specimen was found approximately 30 m (100 ft) above river level in a clear sandstone (1953 field notes, CMN archives). CMN 8920 was first described by Russell (1956) as pertaining to *Champsosaurus nator* Parks, 1933, but was reassigned to the newly erected *C. lindoei* Gao & Fox, 1998, based on its relatively small size (approximately 24.3 cm basioccipital length), gracile snout, expanded narial bulla, weak pterygoid flange, and strait inferior temporal arch.

CMN 8920 was scanned at UTCT with a voxel size of 60.5 µm, at 200 kV, and 0.3 mA. This produced 4579 slices, which were converted to 8-bit tiff files for segmenting. The dataset was divided into five subunits, where every other tiff file within each subunit was selected for loading into Amira 5.4.3 to perform visualization and segmentation using the LabelFields module. Elements of the cranium were segmented individually and rendered using the SurfaceView module. The surface models of each subunit were then recombined, creating a colour-coded model of the complete skull for manipulation and description. The 3D models generated from this study are available online via MorphoSource (https://www.morphosource.org/Detail/MediaDetail/Show/media_id/46683).

Results

Overall skull morphology

CMN 8920 is a remarkably complete skull, lacking jaws, that has been subject to only slight post-mortem and taphonomic modifications (Figs 1–3): crushing of the right squamosal and quadratojugal; the posterior tips of the opisthotics and parasphenoid have broken away; the premaxillae, maxillae, nasal, internarial and prefrontals are fractured and have been infilled with matrix; and the tip of the rostrum is twisted counter-clockwise when the skull is viewed anteriorly.

The length of CMN 8920 is typical for an adult-sized skull of *C. lindoei* (Table 1; Fig. 4) and is similar in overall morphology to other specimens reported by Gao & Fox (1998). As is characteristic for choristoderes, the skull is dorsoventrally flattened, with prominent temporal arches that expand posterolaterally and give the skull a cordiform dorsal profile. The nares are confluent and open anteriorly on the snout, as is seen in many choristoderes (Gao & Fox, 1998).

Dermatocranium

Premaxilla

Both premaxillae are preserved (Fig. 5A), although they have both undergone slight fragmentation. When viewed dorsally, the paired premaxillae form a rounded nasal bulla that is wider than the anterior-most extent of the maxillae. The premaxillae are prevented from contacting one another posterodorsally by an invasion of the nasal. This condition is mirrored ventrally, where the premaxillae are separated from one another by the internarial posterior to the incisive foramina. The premaxilla contacts the maxilla immediately posterior to the seventh tooth position with a suture that runs relatively perpendicular to the long axis of the snout. Together, the premaxillae nearly completely surround the narial opening, which opens onto the anterior surface of the snout. The dorsal rim of the narial opening does not extend as far forward as the ventral rim, causing the narial opening to face slightly dorsally.

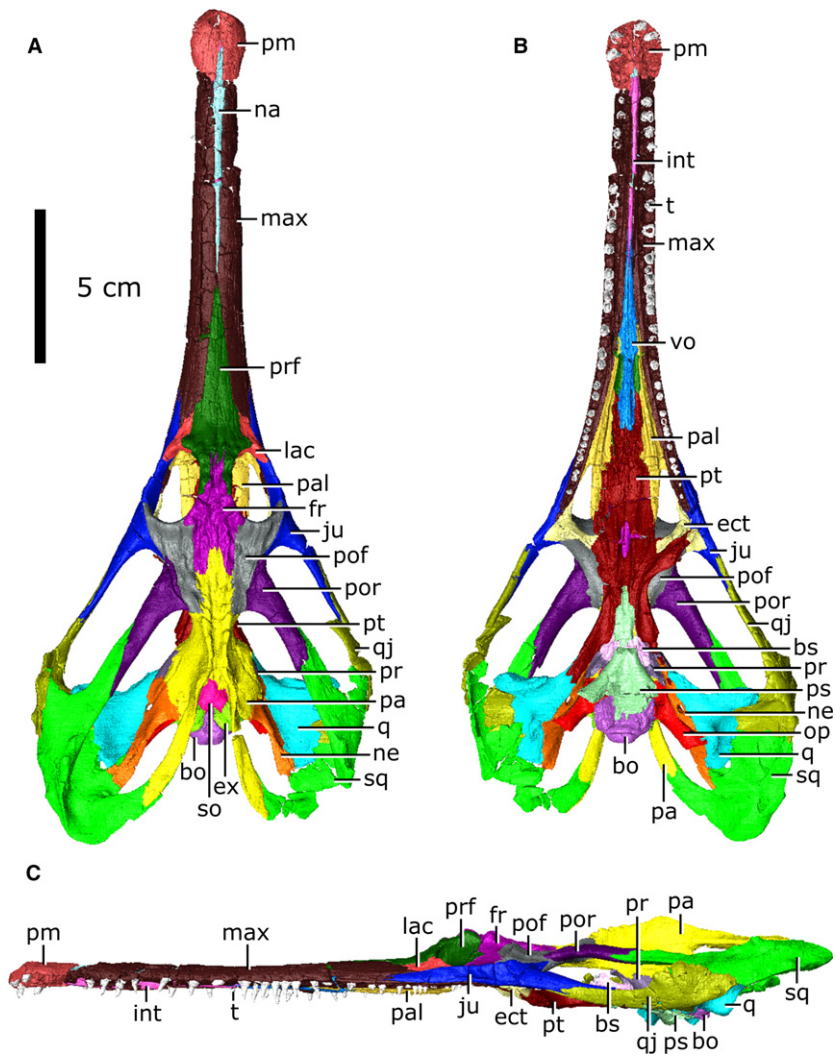


Fig. 1 Articated skull of *Champsosaurus lindoei* (CMN 8920). (A) dorsal view; (B) ventral view; (C) lateral view.

Internally these elements possess a network of canals that run from foramina on the external surface (Fig. 5A; CN V₂f) into a large tract that runs the entire length of the snout. This canal likely carried the maxillary branch of the trigeminal nerve (CN V₂), and these foramina, therefore, would have held sensory nerves that innervated the snout. The medial surface of the premaxilla indicates that the anterior region of the nasal vestibule was smooth, lacking any evidence of conchae.

Maxilla

Both maxillae are preserved (Fig. 5B), but are highly fragmented anteriorly. In lateral view, the maxilla is elongate and dorsoventrally thin, extending from the seventh tooth position to the ectopterygoids (Fig. 1B). The maxillae only briefly contact one another at the midpoint of the dorsal surface of the snout, where the nasal and prefrontals taper towards one another. On the dorsal surface, the maxillae are separated by the nasal anteriorly and the prefrontals posteriorly, and vanish from external view posteriorly at the

suture with the lacrimal. On the ventral surface, the maxillae are separated anteriorly by the internarial and vomers. Ventromedially, the maxilla contacts the palatine for the entire length of the latter, extending from the anterior margin of the choana to the midpoint of the suborbital fenestra, terminating anterior to the ectopterygoid.

Like the premaxilla, the maxilla is smooth externally, but punctured by dozens of foramina scattered across its surface (Fig. 5B; CN V₂f). These foramina penetrate the maxilla and commune with the canal for CN V₂ that extends the entire length of the maxilla. However, the maxilla only surrounds the canal completely for the anterior half of its length; the posterior half of the maxilla comprises only the dorsolateral wall of the CN V₂ canal. The maxilla surrounds the nasal vestibule for the anterior half of its length, before diverging laterally away from the nasal passage.

Nasal

The nasals are elongate and fused with no identifiable suture, and will therefore be treated as a single element

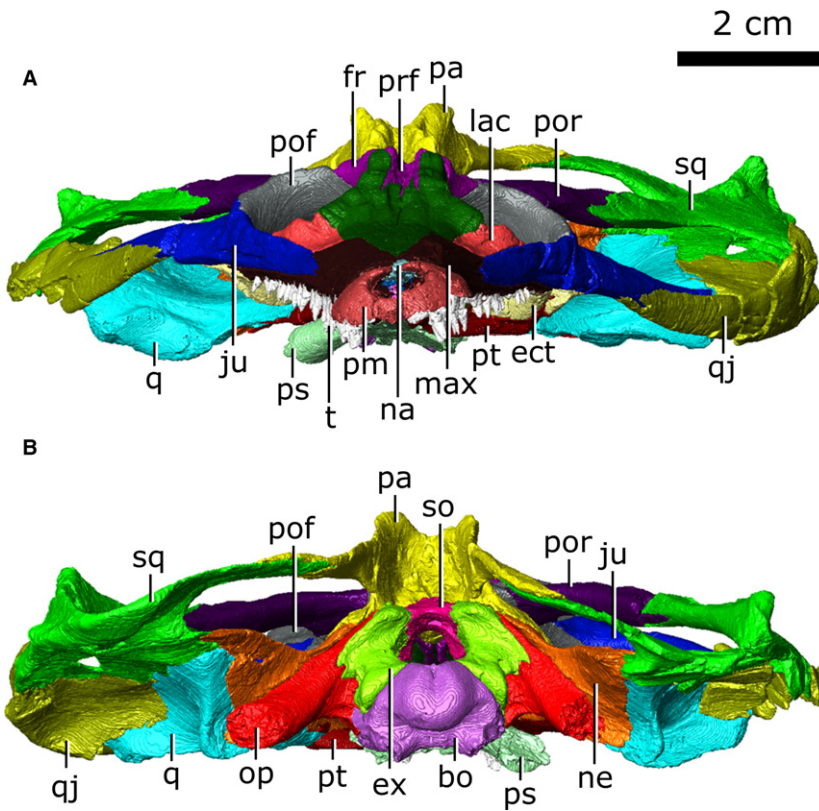


Fig. 2 Articulated skull of *Champsosaurus lindoei* (CMN 8920). (A) anterior view; (B) posterior view.

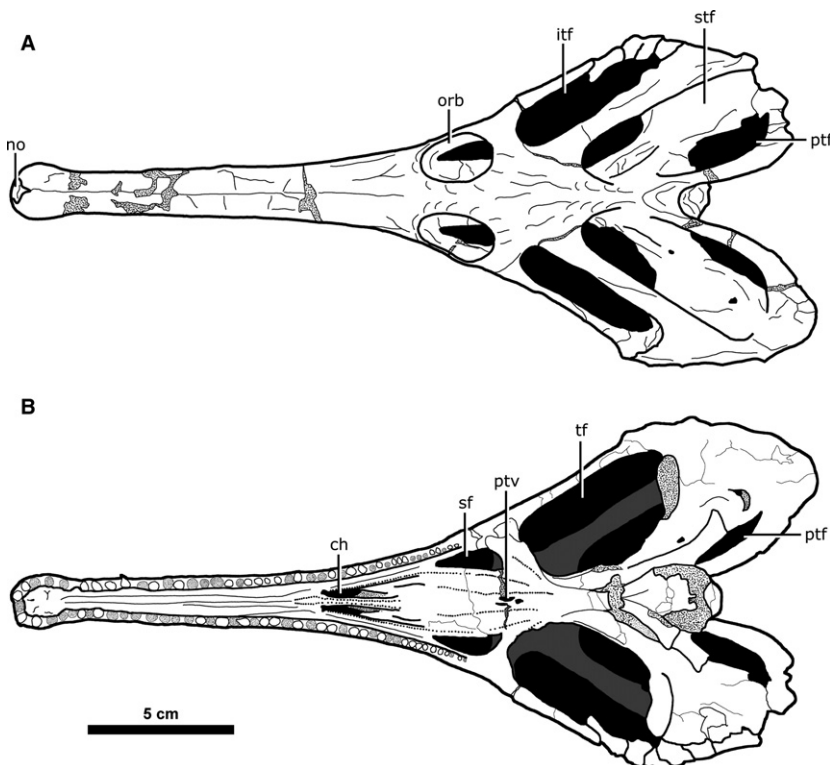


Fig. 3 Major skull openings of *Champsosaurus lindoei* (CMN 8920). (A) dorsal view; (B) ventral view.

(Fig. 6A). In dorsal view, the nasal is slender and elongate, narrowing as it extends posteriorly. The anterior-most portion is fragmented and poorly preserved, and as a result,

this element does not contact the narial opening; however, it is likely that the nasal would contact the narial opening when intact, as indicated by the medial suture of the

Table 1 Measurements for the skull of *Champsosaurus lindoei* (CMN 8920).

Measurement	Value(s), mm; left/right
1 Basal skull length	243
2 Maximum skull length	278
3 Skull width at quadratojugals	113
4 Snout length (anterior of orbits)	147
5 Width of snout base	33
6 Width of distal snout posterior to bulla	14
7 Width of bulla	20
8 Maximum orbital length	25/24
9 Maximum orbital width	17/17
10 Interorbital width	11
11 Maximum infratemporal fenestra length	55/54
12 Maximum infratemporal fenestra width	16/16
13 Maximum supratemporal fenestra length	66/66
14 Maximum supratemporal fenestra width	26/26
15 Width of parietal table	34
16 Length of parietal table (posterior to orbits)	49
17 Nares length (anteroposterior)	5
18 Nares width	7
19 Anteroposterior length of maxillary tooth row	164

premaxillae, and the condition seen in other more complete specimens (Erickson, 1972). The nasal extends anteriorly between the premaxillae and terminates between the anterior projections of the prefrontals posteriorly, ventral to the outer surface of the maxillae. A thin projection (approximately 1 mm high; Fig. 6A; vpn) extends ventrally along the entire length of the nasal towards the internarial, suggesting a cartilaginous wall may have separated the nasal passages for at least the anterior portion of the nasal passage.

Lacrimal

Both lacrimals are perfectly preserved (Fig. 6B). The lacrimal is a relatively small element on the dorsal surface of the snout that comprises the anterior-most margin of the orbits. It is triangular when viewed dorsally and is bordered by the maxilla anteriorly, the prefrontal medially, the jugal

laterally, and the palatine ventrally. The computed tomography (CT) data reveal a triangular, striated shelf (Fig. 6B; lshf) that projects deep to the maxilla anteriorly, making the extent of this element nearly twice as large as that seen on the surface. The surface of the lacrimal becomes rugose anterior to the orbit, resembling the ornamentation seen on the prefrontal, frontal and parietal.

The ventral surface of the lacrimal forms the dorsomedial wall of the nasolacrimal canal that opens posteriorly into the orbit. The CT data show that this canal opens anteriorly into the nasal passage through a small gap (0.8 mm high by 4 mm long) between the maxilla and palatine, supporting the interpretation of Russell (1956). Interestingly, the canal continues anterior to this gap and extends through the maxilla and premaxilla to the very tip of the snout, with branches towards the outer surface of the skull, as is typical of CN V₂. This morphology suggests that the nasolacrimal canal was confluent with CN V₂ in *Champsosaurus*, a feature that is also observed in other species of *Champsosaurus* (e.g. *C. natator*; Russell, 1956) and possibly other neochoristoderes (e.g. *Tchoiria namsarai*; Ksepka et al. 2005). There is no other duct connecting the orbit to the nasal passage in *Champsosaurus*, and this is therefore the only canal that could have possibly carried the nasolacrimal duct.

Prefrontal

Both prefrontals are well-preserved with little fracturing and distortion (Fig. 7A). Anteriorly, the prefrontal sits medial to the lacrimal and maxilla, where the prefrontal forms a large triangular projection when viewed dorsally. This projection penetrates the maxilla before terminating near the midpoint of the snout, at the posterior extent of the nasal. The prefrontals contact for approximately 80% of their length, forking laterally around the frontals posteriorly, and form the rugose anteromedial rim of the orbit. The elongate and highly interdigitated prefrontal–frontal suture is obscured on the surface by ornamentation, but is clearly visible on the CT data. On the ventral surface, the anterior portion of the prefrontal forms the roof of the nasal vestibule that expands posteriorly to form the body of the olfactory chamber (Fig. 7A; och). The chamber narrows

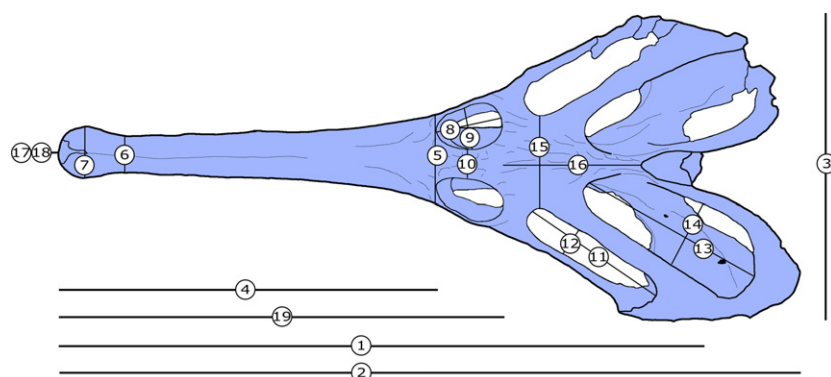


Fig. 4 Skull measurements for *Champsosaurus lindoei* (CMN 8920). See Table 1 for corresponding measurement descriptions and values.

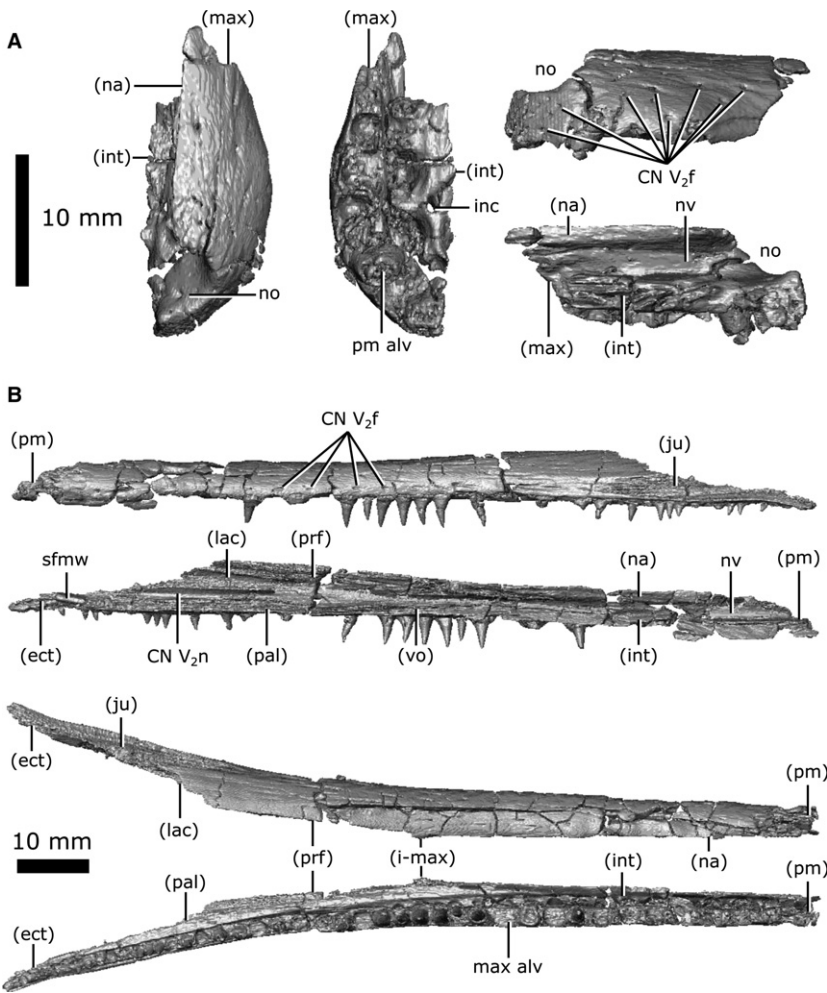


Fig. 5 Isolated premaxilla and maxilla of *Champsosaurus lindoei* (CMN 8920). (A) left premaxilla in dorsal view (left), ventral view (middle), lateral view (top right), medial view (bottom right); (B) left maxilla in lateral view (top), medial view (second from top), dorsal view (second from bottom), ventral view (bottom).

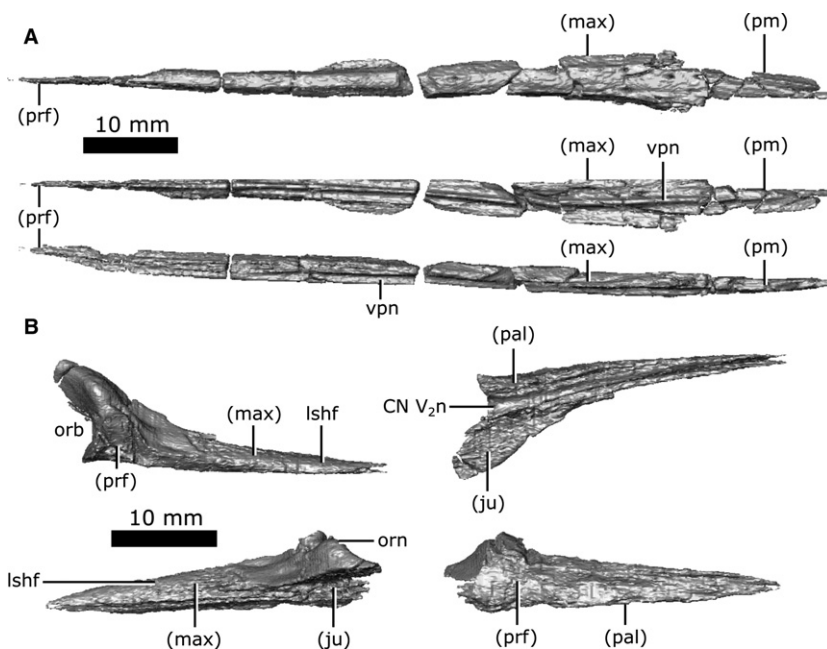


Fig. 6 Isolated nasal and lacrimal of *Champsosaurus lindoei* (CMN 8920). (A) nasal in dorsal view (top), ventral view (middle), right lateral view (bottom); (B) left lacrimal in dorsal view (top left), ventral view (top right), lateral view (bottom left), medial view (bottom right).

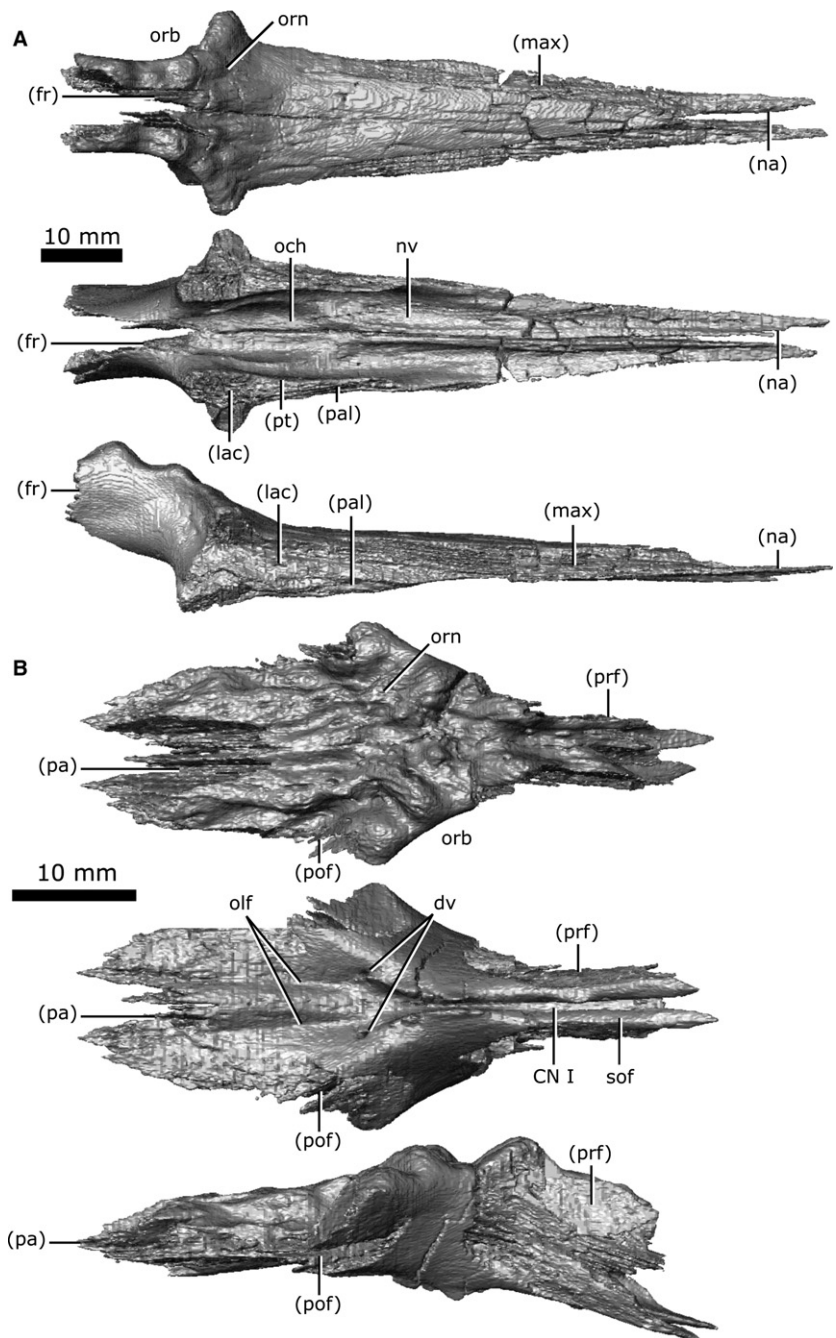


Fig. 7 Isolated prefrontals and frontals of *Champsosaurus lindoei* (CMN 8920). (A) prefrontals in dorsal view (top), ventral view (middle), right lateral view (bottom); (B) frontals in dorsal view (top), ventral view (middle), right lateral view (bottom).

posteriorly to commune with the olfactory duct (CN I) housed by the frontals. Ventrolaterally, the prefrontal contacts the palatine with a suture that extends from the choana to the orbit. The prefrontal contacts the pterygoid along the ventral-most portion of the walls of the olfactory chamber, although it cannot be determined if this contact is genuine or attributable to crushing of the pterygoid.

Frontal

Both frontals are well-preserved and complete, and together are roughly rhomboid when viewed dorsally (Fig. 7B). The dorsal surface of the frontal is rugose,

possessing the most prominent cranial ornamentation on the skull, and composes the posteromedial portion of the orbits. The frontal is bordered anteriorly by the prefrontal, laterally by the postfrontal, and posteriorly by the parietal, which penetrates the frontals in a wide V-shaped suture when viewed dorsally. The CT data show that the frontoparietal suture has a complex internal structure, with a high degree of interdigitation. The subolfactory flanges (Fig. 7B; sof) on the ventral surface of the frontals wrap around the olfactory duct (CN I) but do not completely enclose it, and the duct remains open ventrally. This duct extends from the frontal–prefrontal suture to the midline

of the posterior rim of the orbits. At this point, the duct opens and communicates with the olfactory stalk of the brain, represented by two shallow, parallel troughs extending from the posterior opening of the olfactory duct, along the ventral surface of the frontals and parietals to the mid-brain. Two foramina can be seen leading into the ventral surface of the frontals in the impression left by the anterior-most extent of the olfactory stalks. The CT data reveal that these foramina fork and dissipate into the cortical bone of the frontals, suggesting that they are vascular and carried diploic veins (Witmer & Ridgely, 2009).

Postfrontal

Both postfrontals are preserved with only slight fragmentation, and are triangular in dorsal view (Fig. 8A). The dorsal surface of the postfrontal has slight pitting, although it is modest compared to the ornamentation of the frontal, prefrontal or parietal. The anterior margin of the postfrontal forms the posterior rim of the orbit and is separated from its counterpart by the frontals anteromedially, and the parietals posteromedially. The postfrontal borders the jugal laterally and the postorbital posterolaterally, and forms a portion of the anterior border of both the supratemporal and infratemporal fenestrae.

Postorbital

The postorbitals are well-preserved (Fig. 8B), with a slight amount of fragmentation, particularly on the right

element. In dorsal view, the postorbital is roughly cylindrical and forms the anterior portion of the superior temporal arch. The right postorbital shares a small suture with the right jugal at its anterior-most extent. Anteriorly, it contacts the postfrontal, but the postorbitals have no contact with the orbits. The postorbital usually contacts the orbits in other tetrapods, but the arrangement seen in CMN 8920 is typical for *Champsosaurus* (Gao & Fox, 1998). The suture with the postfrontal is badly damaged on both sides, having cracked along the length of the suture and infilled with sediment. Posteriorly, the postorbital contacts the squamosal via a suture along the length of the superior temporal arch.

Parietal

Both parietals are well-preserved (Fig. 9), with significant fragmentation only occurring along the post-temporal arch. When viewed dorsally, the parietal is elongate, covering the majority of the length of the brain cavity. The parietal shares a complex suture with the frontal anteriorly and is bordered by the postfrontal anterolaterally. The suture between the parietals lies along the midline of the skull in a depression on the dorsal surface that is bordered laterally by an ornamented ridge. The parietals extend laterally over the dorsal portion of the neomorph, as well as the body of the opisthotic and the posterior portion of the prootic. Posteriorly, the parietals extend along the post-temporal arch (Fig. 9; pta) to contact the squamosal. The parietal forms

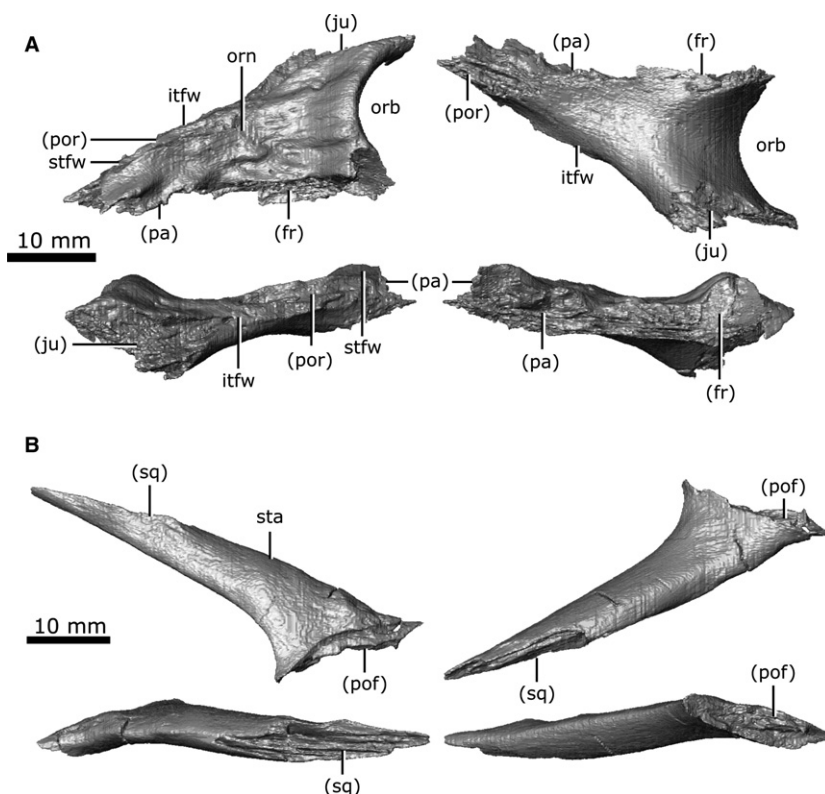


Fig. 8 Isolated postfrontal and postorbital of *Champsosaurus lindoei* (CMN 8920). (A) left postfrontal in dorsal view (top left), ventral view (top right), lateral view (bottom left), medial view (bottom right); (B) left postorbital in dorsal view (top left), ventral view (top right), lateral view (bottom left), medial view (bottom right).

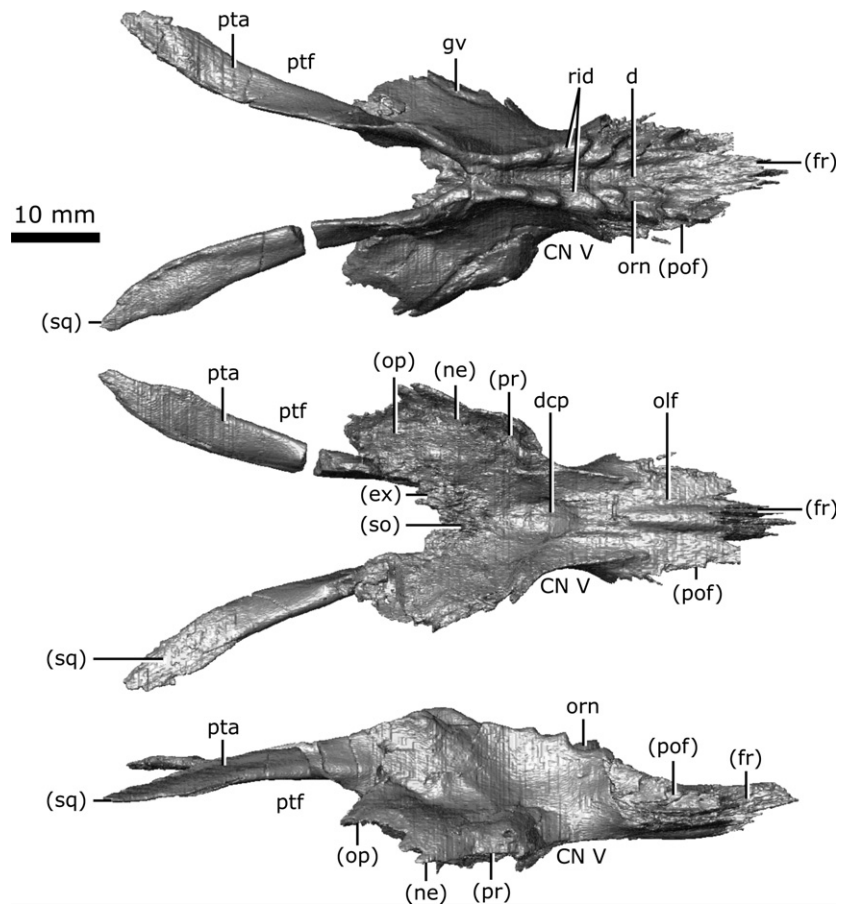


Fig. 9 Isolated parietals of *Champsosaurus lindoei* (CMN 8920) in dorsal view (top), ventral view (middle), right lateral view (bottom).

approximately half of the post-temporal arch, and forms the dorsal rim of the post-temporal fenestra.

A distinct groove is seen on the lateral surface of the parietal (Fig. 9; gv) that extends from the opening for CN V, onto the lateral surface of the neomorph, and terminates at the rim of the pterygoquadrate foramen. Russell (1956:11) described a 'low but distinct ridge' extending anteroventrally along the lateral surface of the parietal that presumably represented the demarcation between the small anterior and large posterior portions of the temporal muscles. This ridge is absent on CMN 8920, consistent with previous observations (Gao & Fox, 1998) that this ridge tends to be less prominent in smaller *Champsosaurus* such as *C. lindoei*. The ventral surface of the parietal over the braincase is concave (Fig. 9; dcp), and housed the large dorsal expansion of the pineal body, although there is no evidence for a pineal opening in *C. lindoei*. The ventral surface of the parietal anterior to the concavity for the pineal body is striated with vascular sulci, suggesting that the dura mater pressed close to the bone in life. Anterolateral to the dorsal concavity of the parietal, the lateral edge of the parietal forms the dorsal rim of the exit for CN V. The concave ventral surface of the parietal continues posteriorly for the rest of its length, where it roofs the opisthotic and exoccipital laterally, and the supraoccipital medially.

Neomorph

The neomorphic bone was first identified by Fox (1968) as a small triangular bone when viewed laterally, having previously been identified as part of the squamosal (Brown, 1905) or prootic (Fox, 1968). The exact extent of this element was poorly understood, and was simply described as bordering the prootic, parietal and pterygoquadrate foramen (Fox, 1968). In the first description of *C. gigas*, Erickson (1972) stated that there was no evidence for a neomorphic element, and that this bone was simply an extension of the parietal. This interpretation was refuted by Gao & Fox (1998), who described the neomorph as an elongate element extending posterior to the pterygoquadrate foramen that appears to share an extensive dorsal suture with the parietal. The data reported in the present study support Fox's (1968) hypothesis that the neomorphic element is a distinct ossification and follows a morphology similar to that proposed by Gao & Fox (1998).

Both left and right neomorphic elements are well-preserved in CMN 8920, with fracturing only occurring in the dorsal region near the juncture with the parietals.

The neomorph is an elongate ossification when viewed laterally, extending along the entire medial surface of the quadrate, and sits lateral to the braincase without contacting the brain cavity or endosseous labyrinth (Fig. 10). At its anterior extent, a projection of the neomorph penetrates

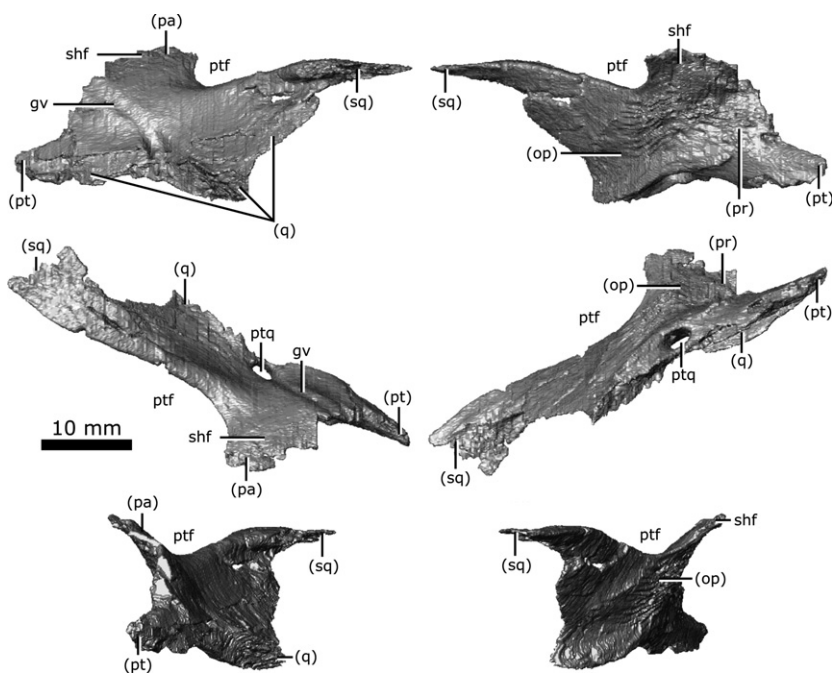


Fig. 10 Isolated left neomorph bone of *Champsosaurus lindoei* (CMN 8920) in lateral view (top left), medial view (top right), dorsal view (middle left), ventral view (middle right), anterior view (bottom left), posterior view (bottom right).

the quadrate ramus of the pterygoid. The neomorph extends posteriorly, ventral to the parietal and dorsolateral to the prootic and opisthotic. The CT data reveal for the first time a short tapering shelf (Fig. 10; shf) that extends dorsally underneath the parietal for the entirety of its shared suture with the neomorph. A distinct groove (Fig. 10; gv) extends along the dorsal surface of the neomorph from the parietal to the pterygoquadrate foramen (Fig. 10; ptq). This groove has been illustrated in *C. gigas* (Erickson, 1972) and *C. natator* (Fox, 1968), and is presumed to be common to *Champsosaurus*. The neomorph contacts the quadrate laterally, extending posterodorsally in a long and slender projection to meet the squamosal. The neomorph forms almost the entire ventral rim of the post-temporal fenestra. Contrary to previous interpretations (e.g. Gao & Fox, 1998), the pterygoquadrate foramen is completely encompassed by the neomorph bone.

Jugal

Both jugals are preserved with some fragmentation around the orbits and along the inferior temporal arch (Fig. 11A). The jugal is long and slender when viewed laterally. It contacts the maxilla anteriorly by a long, thin projection, and contacts the lacrimal dorsally along the length of this projection. The jugals share a short suture with the palatine near the opening for the CN V₂ canal and the nasolacrimal duct. The jugal comprises the most lateral portion of the orbits, posterior to its contact with the lacrimal. The jugal shares a suture with the postfrontal, which extends from the posterolateral portion of the orbit to the anteromedial portion of the infratemporal fenestra. The right jugal has a small contact with the right postorbital (approximately

1 mm long), but the left jugal terminates immediately anterior to the postorbital. The jugal extends posterolaterally to form the gracile inferior temporal arch, along with the anterior portion of the quadratojugal. The jugal-quadratojugal suture is long, extending for the majority of the length of the inferior temporal arch (Fig. 11A; ita). This arch is straight, giving the infratemporal fenestra a rectangular profile, as is typical for *C. lindoei* (Gao and Fox, 1998). This differentiates the species from the contemporaneous *C. natator*, which possesses an inferior temporal arch that is bowed outwards (Gao & Fox, 1998).

Quadratojugal

Both quadratojugals are preserved; the right one is heavily fragmented but the left one remains intact (Fig. 11B). When viewed laterally, the quadratojugal is elongate and widens posterior to the inferior temporal arch. The quadratojugal forms the lateral-most portion of the temporal region, with only minimal ornamentation on the lateral surface. It contacts the jugal anteriorly via a long suture and expands posteroventrally to form the anteroventral portion of the temporal region. Here, the quadratojugal contacts the squamosal dorsolaterally and posteriorly via a long, thin suture. The quadratojugal also contacts the quadrate medially, immediately lateral to the articular surface for the jaws.

Squamosal

Both squamosals are preserved in CMN 8920, but the right is fragmented such that morphological interpretation must be based entirely on the left element. The squamosal is large in relation to the other cranial elements (Fig. 11C), with ornamentation on the posterolateral, lateral and

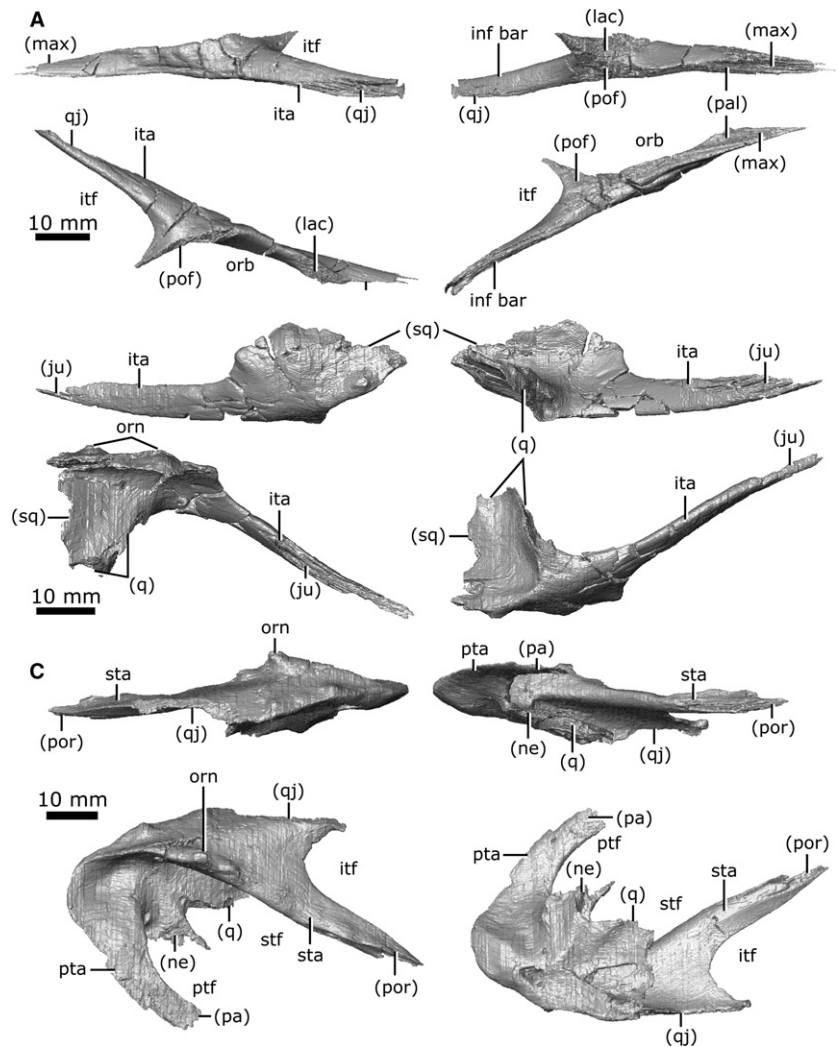


Fig. 11 Isolated jugal, quadratojugal, and squamosal of *Champsosaurus lindoei* (CMN 8920). (A) left jugal in lateral view (top left), medial view (top right), dorsal view (bottom left), ventral view (bottom right); (B) left quadratojugal in lateral view (top left), medial view (top right), dorsal view (bottom left), ventral view (bottom right); (C) left squamosal in lateral view (top left), medial view (top right), dorsal view (bottom left), ventral view (bottom right).

dorsal surfaces. When viewed laterally, the squamosal is long and dorsoventrally flat. This element forms the posterior margin of the supratemporal fenestrae and gives the skull its stereotypical cordiform profile. Anterolaterally, the squamosal shares a suture with the quadratojugal, beginning posterior to the inferior temporal arch and extending posterior to the ventral truncation of the superior temporal arch. The squamosal extends anteromedially along the superior temporal arch (Fig. 11C; sta) where it contacts the postorbital in an elongated suture. Ventromedially it contacts the quadrate, and the posterolateral projection of the neomorph. The squamosal forms the dorsolateral rim of the post-temporal fenestra, and contacts the parietal along the post-temporal arch (Fig. 11C; pta).

Vomer

Both vomers are present and have experienced significant fracturing throughout (Fig. 12A). In ventral view, the vomer is triangular in profile. The vomer originates anteriorly as a slender projection within the internarial, but expands

posteriorly, becoming exposed on the ventral surface. As it extends posteriorly, it widens laterally and contacts the maxilla and the anterior projection of the palatine laterally, before separating from them to form the medial wall of the choana. At its posterior extent, it contacts the pterygoid laterally, before terminating with a short, wedge-shaped projection that extends ventral to the pterygoid. A single row of vomerine teeth are present that run the length of the ventral surface and enlarge posteriorly (Fig. 12A; vom alv). The CT data show a distinct ridge (approximately 1 mm high) that extends dorsally from each vomer into the nasal passage, and likely represents the paired vomerine septum (Fig. 12A; vs). These projections become enlarged posteriorly (approximately 1.8 mm high), curling medially, although some of this curling may be attributable to breakage post-mortem.

Palatine

Both palatines are well-preserved (Fig. 12B), with fracturing only occurring on the posterior process that

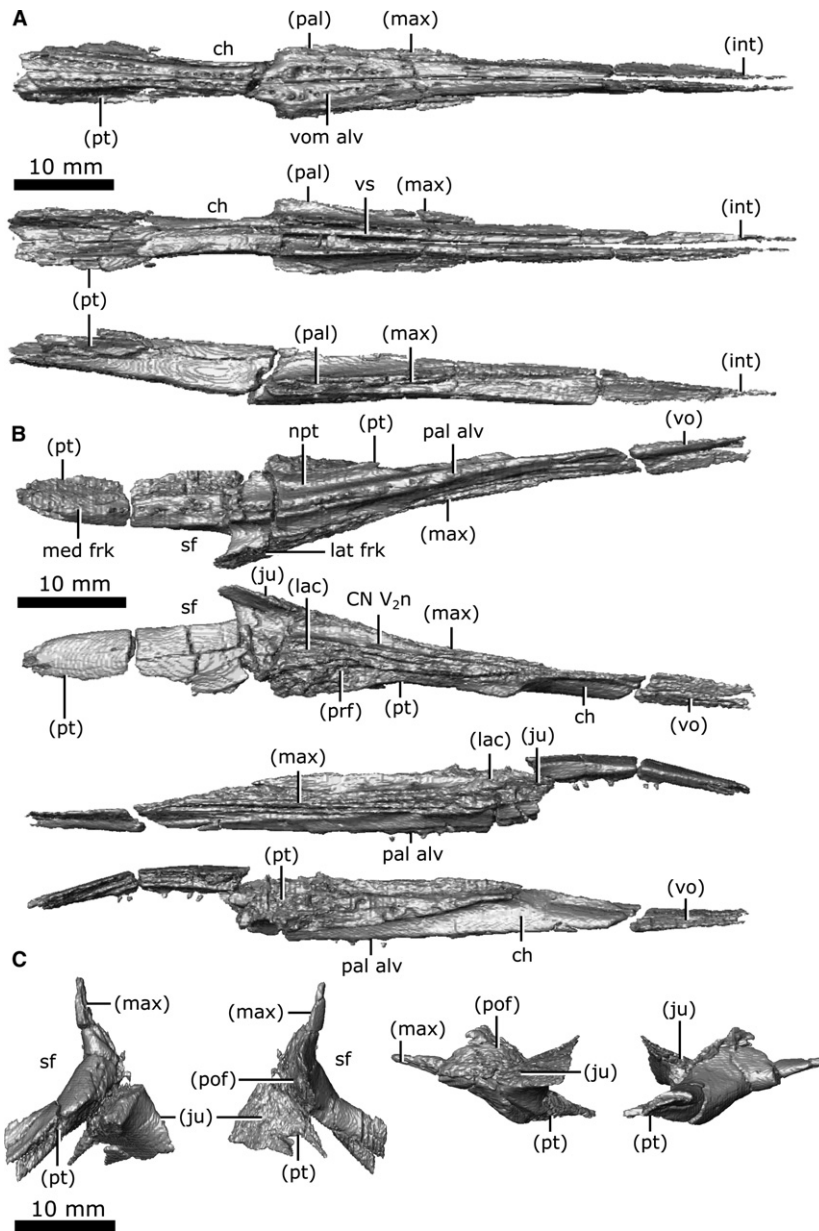


Fig. 12 Isolated vomers, palatine, and ectopterygoid of *Champsosaurus lindoei* (CMN 8920). (A) vomers in ventral view (top), dorsal view (middle), right lateral view (bottom); (B) left palatine in ventral view (top), dorsal view (second from top), lateral view (second from bottom), medial view (bottom); (C) left ectopterygoid in ventral view (left), dorsal view (second from left), lateral view (second from right), medial view (right).

borders the suborbital fenestra. In ventral view, the palatine is triangular, elongate and thin, comprising the lateral portion of the palate posteriorly and the anteromedial wall of the suborbital fenestra. A single row of palatine teeth (Fig. 12B; pal alv) runs the entire length of this element along a ridge that continues posteriorly onto the pterygoid. The nasopalatal trough (Fig. 12B; npt) extends the length of the palatine on the ventral surface and continues posteriorly onto the pterygoids. This trough is shallow in CMN 8920 compared with those of other *Champsosaurus* specimens (e.g. TMP 87.36.41, TMP 94.163.01, TMP 86.12.11, CMN 8919; Matsumoto & Evans, 2016), likely due to crushing of the palatal region.

The palatine originates anteriorly between the vomer medially and the maxilla laterally, before separating from the vomer to form the lateral rim of the choana. Posterior to the choana, the palatine contacts the pterygoid medially, and remains wedged between this element and the maxilla for the majority of its length. Extending posteriorly, it forks around the suborbital fenestra, where the shorter lateral fork contacts the maxilla laterally and a small portion of the jugal dorsally, and the longer medial fork contacts the pterygoid. Posterior to the choana, the palatine contacts the prefrontal and lacrimal dorsally, and these bones remain in contact with one another until the anterior rim of the orbit, where they separate. The dorsal surface of the palatine forms the floor of the common canal for CN V₂

(laterally) and the nasolacrimal duct (medially; Fig. 12B; CN V_{2n}).

Ectopterygoid

Both ectopterygoids are well-preserved with little to no fracturing or distortion (Fig. 12C). When viewed ventrally, the ectopterygoids are short and pillar-like and articulate with the lateral-most extent of the pterygoid flange, as reported previously by Erickson (1972) and Gao & Fox (1998). This element forms the posterior wall of the suborbital fenestra and separates it from the temporal fossa. The suture between the ectopterygoid and the pterygoid is well ossified and indistinct on the external surface. The suture is only visible intermittently along its length in the CT scan, and the remainder of the suture had to be interpreted. The well-fused suture has been reported before by Erickson (1972) who described it as heavily ankylosed, and by Gao & Fox (1998) who were able to identify the suture on the right side of TMP 87.36.41, but not the left. The ectopterygoid contacts the pterygoid posteromedially, the jugal laterally, the postfrontal dorsolaterally, and the posterior tip of the maxilla anterolaterally. Erickson (1972) described a ridge on the ventral surface of the pterygoid flange that extends onto the ectopterygoid, but these CT data reveal that the ridge is only present on the pterygoid flange, adjacent to the suture between the pterygoid and the ectopterygoid.

Pterygoid

Both pterygoids are preserved and complete, but they have experienced heavy fragmentation in the anterior palatal region (Fig. 13). In ventral view, the pterygoids form a large plate of bone that comprises the majority of the surface of the palate. It contacts the vomer anteromedially and the palatine anterolaterally, and forms the posteromedial wall of the suborbital foramen. It expands posteriorly to form the floor of the olfactory chamber where it appears to share a slender contact with the prefrontals laterally, although it cannot be determined if this contact is genuine or due to displacement of the element by crushing. The pterygoid usually forms a dorsal concavity in the palate of *Champsosaurus* (Erickson, 1985), but this feature is exacerbated in CMN 8920 by crushing (Fig. 13; dc). The nasopalatal troughs run along the anterior half of the ventral surface of the pterygoid (Fig. 13; npt), and are bordered on each side by rows of palatal teeth (Fig. 13; pt alv). These troughs are indistinct across their anterior halves, possibly due to crushing of the palatal region.

A distinct flange extends laterally from the pterygoid along the anterior wall of the temporal fossa and posterior surface of the ectopterygoid (Fig. 13; ptf). Previously (Erickson, 1972), this flange, along with the ectopterygoid, have been identified together as the pterygoid flange due to the high degree of ossification between these elements, but it can be seen here that the true pterygoid flange is actually

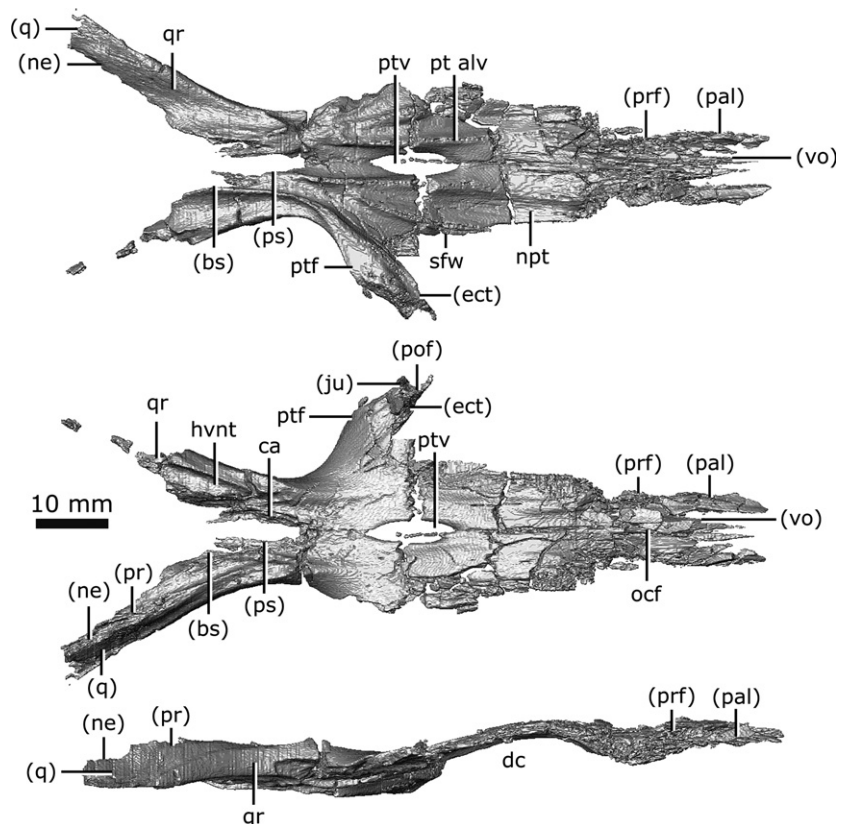


Fig. 13 Isolated pterygoids of *Champsosaurus lindoei* (CMN 8920) in ventral view (top), dorsal view (middle), right lateral view (bottom).

much more gracile than previously described. The flange has a small contact with the jugal and postfrontal at its dorsolateral margin. Medial to the pterygoid flange, the pterygoids briefly separate from one another to form the interpterygoid vacuity (Fig. 13; ptv), which has small struts of bone extending across it. Russell (1956) interpreted the interpterygoid vacuity as resulting from incomplete ossification, but the presence of this feature in other, larger specimens suggests that this vacuity does not ossify in *Champsosaurus*. Russell (1956) suggested the struts of bone across the interpterygoid vacuity in CMN 8920 were evidence of incomplete ossification, but the CT data reveal they are due to breakage of the pterygoid.

The pterygoid narrows as it extends posteriorly, forming the medial portion of the temporal fossa. At their narrowest points, the pterygoids are separated from one another by the anterior projection of the parasphenoid. Each pterygoid forks laterally around the parasphenoid, with the carotid artery canal projecting dorsally between them. These lateral forks are the quadrate rami (posterior branches of Russell, 1956; lateral branches of Erickson, 1972; Fig. 13; qr). The quadrate rami extend posteriorly on either side of the basisphenoid, forming a trough on each side of the braincase that housed the lateral head vein. The quadrate ramus forms the ventral and lateral walls of the lateral head vein trough (Fig. 13; hvnt), and the basisphenoid forms the medial wall. The ramus extends posteriorly to briefly contact the prootic dorsally and the anterior-most portion of the quadrate. The ramus becomes wedged between the quadrate dorsolaterally and the neomorph dorsomedially, only being exposed on the ventral surface. The quadrate ramus envelops the anterior projection of the neomorph, obscuring the projection from external view. The quadrate ramus terminates posteriorly at the mid-length of the fenestra ovalis.

Dentition

A single row of marginal teeth runs along the premaxilla and maxilla, posteriorly terminating ventral to the mid-length of the orbit (Fig. 13C). There are six alveoli on the premaxilla, and 41 on the maxilla, resulting in a total of 94 alveoli, of which 62 have teeth at least partially preserved. No replacement teeth were identified in this individual. The marginal teeth are sub-theodont and conical (Fig. 14). Previous descriptions of *Champsosaurus* (Matsumoto & Evans, 2016) reported the marginal teeth as having plicidentine, with visible longitudinal striations in the enamel. These striations are not apparent on the maxillary teeth of CMN 8920, but the CT data show internal plicidentine infolding. This infolding is only present near the base of the tooth and vanishes apically. No premaxillary teeth are completely preserved in CMN 8920, but plicidentine infolding is seen internally near the base of the fragmentary premaxillary teeth. Overall, the marginal teeth show a trend of decreasing size posteriorly (6 mm at 21st alveoli, 2 mm at 47th alveoli), a trend that is consistent with previous descriptions

of *Champsosaurus* and other neochoristoderes (Matsumoto & Evans, 2016).

Distinct rows of fine palatal teeth are seen on the pterygoids, palatines and vomers, giving these elements a sandpaper-like texture ventrally (Fig. 14D; red areas). Rows of palatal teeth on the palatine, vomer and pterygoid border the nasopalatal trough as it extends posteriorly from the choana. All palatal teeth are either broken or have fallen out, but have been described as conical and unstriated in other specimens of *C. lindoei* (Matsumoto & Evans, 2016). Like the marginal teeth, the palatal teeth are also sub-theodont, but differ in that they lack plicidentine infolding.

Splanchnocranium

Quadrate

Both quadrates (Fig. 15) are preserved, but the right has lost the cortical surface on the joint with the articular element of the jaw (Fig. 15; art). When viewed ventrally, the quadrate is large and dorsoventrally flat, forming a broad table ventral to the temporal arches. The quadrate contacts the quadratojugal and squamosal laterally, and the pterygoid, prootic, opisthotic and neomorph medially. Fox (1968) states that the quadrate is firmly bound to both the prootic and opisthotic, but the CT data show that the quadrate is separated from the prootic for the majority of its length by the neomorph. Additionally, the quadrate is separated from the opisthotic by the neomorph, only briefly contacting one another between a small ventral projection (approximately 5 mm long) on the quadrate and the paroccipital process of the opisthotic. The quadrate has a small suture with the pterygoid at its anteromedial-most corner. This suture has been damaged on the left quadrate, but is well-preserved on the right. The right quadrate forms a small portion of the lateral rim of the pterygoquadrate foramen dorsally, but the left quadrate does not contact this opening.

Epipterygoid and Stapes

These elements were not preserved in CMN 8920. Previous descriptions of the epipterygoid in other specimens are reviewed in the Discussion. No stapes has been explicitly described in any choristodere and cannot be commented on at present (but see Discussion for comment on possible choristodere stapes).

Chondrocranium

Internarial

Brown (1905) initially reported this element as the ethmoid and stated that 'the homology of this bone is somewhat questionable'. Russell (1956) and Erickson (1972) reported it as the internarial and described it as a neomorphic ossification that likely derived from the cartilaginous internarial septum. The internarial septum is a component

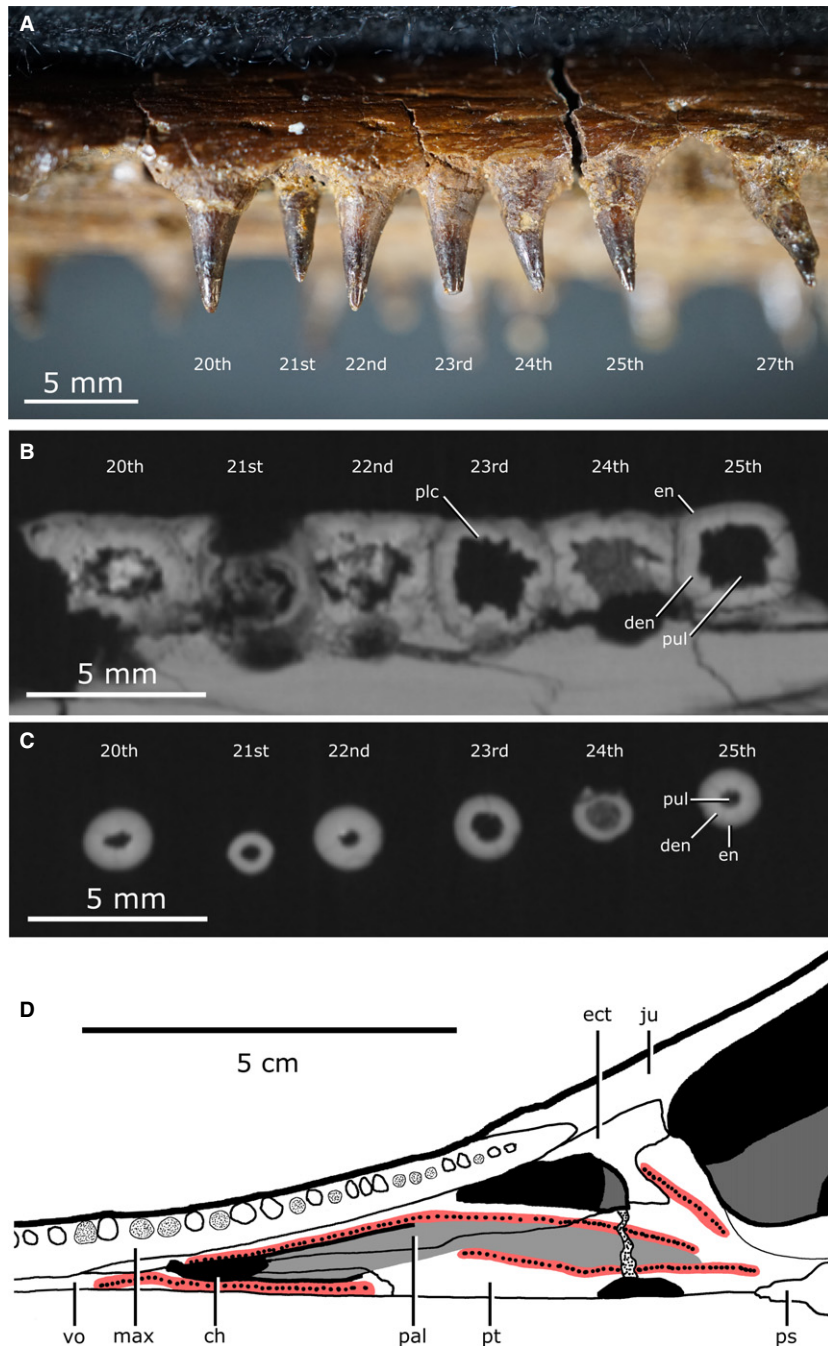


Fig. 14 Tooth morphology of *Champsosaurus lindoei* (CMN 8920). (A) Labial view of left maxillary tooth row; (B) Basal transverse cross section of the maxillary teeth; (C) Apical transverse cross section of the maxillary teeth; (D) Left palatal dentition. Red coloured areas mark the palatal teeth, light-grey coloured area marks the nasopalatal trough.

of the anterior chondrocranium (Bellairs & Kamal, 1981) and the internarial is therefore tentatively included here as a chondrocranial ossification. When viewed ventrally, the internarial is an elongate, midline element that extends along the anterior portion of the mouth roof, separating the paired maxillae and premaxillae (Figs 13B and 16A). It is slightly shorter than the overlying nasal. It originates anteriorly between the paired incisive foramina of the premaxilla and extends posteriorly to terminate between the anterior tips of the vomers. The internarial is not visible anterior to the premaxilla/maxilla suture

because the premaxilla wraps ventrally around the internarial, obscuring it from ventral view. The internarial has a gentle U-shape on the anterior two-thirds of its dorsal surface, forming the floor of the nasal passage (Fig. 16A; U). The posterior third has an elongated ridge (approximately 0.8 mm high; Fig. 16A; dr) extending dorsally into the nasal passage, which is mirrored by a ridge on the ventral surface of the nasal bone above. Together, these elements may have supported the cartilaginous wall that bifurcated the nasal passage, as in extant reptiles (Romer, 1956).

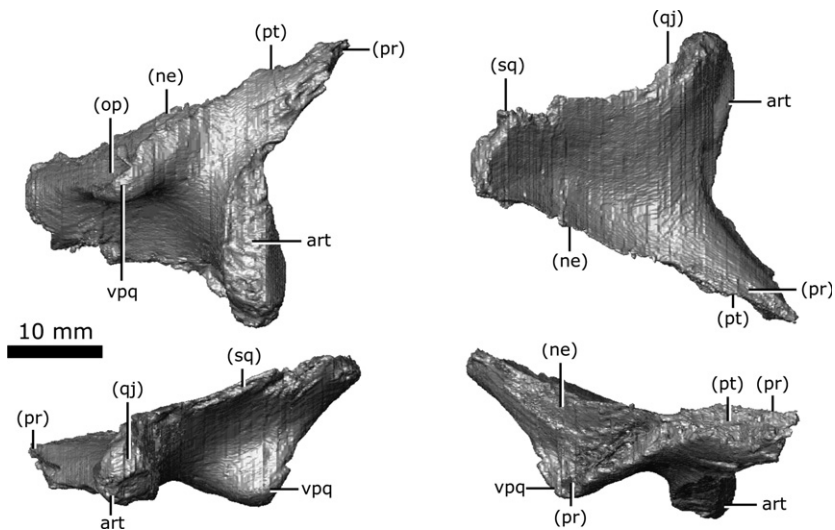


Fig. 15 Isolated left quadrate of *Champsosaurus lindoei* (CMN 8920) in ventral view (top left), dorsal view (top right), lateral view (bottom left), medial view (bottom right).

Prootic

Both prootics are preserved and are slightly fractured (Fig. 16B). Internally, trabecular bone continues to the otic capsule with no surface of cortical bone. The prootic is relatively small (approximately 1.7 cm long) and roughly rhomboid when viewed laterally, forming the anterolateral wall of the fenestra ovalis and otic capsule. The anterior-most rim of the fenestra ovalis is slightly fractured in CMN 8920, but comparisons with other specimens (TMP 87.36.41, TMP 94.163.1) demonstrate that the fenestra ovalis is only slightly smaller when the prootic is intact. It houses the anterior half of the lateral semicircular canal and the anterior portion of the anterior semicircular canal. The prootic forms the posterodorsal rim of the opening for CN V, contacts the parietal posterodorsally, and extends ventrally to contact the basisphenoid, neomorph, pterygoid and quadrate. As it extends posteriorly, it is obscured from external view by the neomorph before terminating at an abrupt, vertically oriented suture with the opisthotic. The facial nerve (CN VII) is interpreted to pass between the basisphenoid and the prootic on the left side, but this nerve exits directly through the prootic on the right, barely contacting the basisphenoid as it exits the skull.

Opisthotic

Both opisthotics are preserved in CMN 8920 (Fig. 16C), which form the posterior portion of the otic capsule, and extend posteriorly to form the paroccipital process (Russell, 1956), giving the opisthotic a cylindrical shape when viewed posteriorly (Fig. 16C; pop). This element originates anteriorly at a vertical suture with the prootic, and borders the neomorph laterally and parietal dorsally. Posteriorly, it expands medially to contact the supraoccipital. The opisthotic forms the posterior wall of the otic capsule, and houses the posterior portions of both the lateral and posterior semicircular canals. A canal extends through the opisthotic from the posterior wall of the otic capsule to the external

posterioventral surface of the opisthotic that we interpret as the pathway for the glossopharyngeal nerve (Fig. 16C; CN IX). Among diapsids, the pathway for CN IX is highly variable, but is often in close association with the otic capsule due to its location within the metotic fissure in development (Bellairs & Kamal, 1981; Rieppel, 1985), and is known to exit through the posterior margin of the otic capsule in other reptiles (Romer, 1956). As the opisthotic continues posteriorly, it becomes separated from the brain cavity by the exoccipital medially, and is bordered by the basioccipital ventrally, the neomorph laterally, and the parietal dorsally. The suture with the exoccipital is obscured internally due to fracturing and partial fusion between these two elements in this area, but all external sutures are clearly visible. The left opisthotic contacts a small portion of the quadrate laterally, but the right does not due to asymmetrical breakage of the paroccipital processes.

Supraoccipital

The supraoccipital is well-preserved with little to no fragmentation or distortion (Fig. 17A). This element roofs the posterior region of the brain cavity, giving it a concave-down profile when viewed posteriorly. The supraoccipital is roofed by the parietals along an interdigitated suture for the majority of its length. The supraoccipital becomes exposed dorsally as the parietals fork laterally to commune with the squamosals. The posterior edge of the supraoccipital forms the dorsal rim of the foramen magnum and is concave when viewed dorsally (Fig. 17A; fm). The supraoccipital contacts the paired prootic, opisthotic and exoccipital laterally. The supraoccipital houses the posterior portion of the anterior semicircular canal (Fig. 17A; ac), the crus communis (Fig. 17A; cc), and the anterior portion of the posterior semicircular canal (Fig. 17A; pc). The supraoccipital, opisthotic and prootic fail to contact one another dorsal to the endosseous labyrinth, forming a cavity that projects dorsally from the pars inferior of the inner ear to reach the ventral

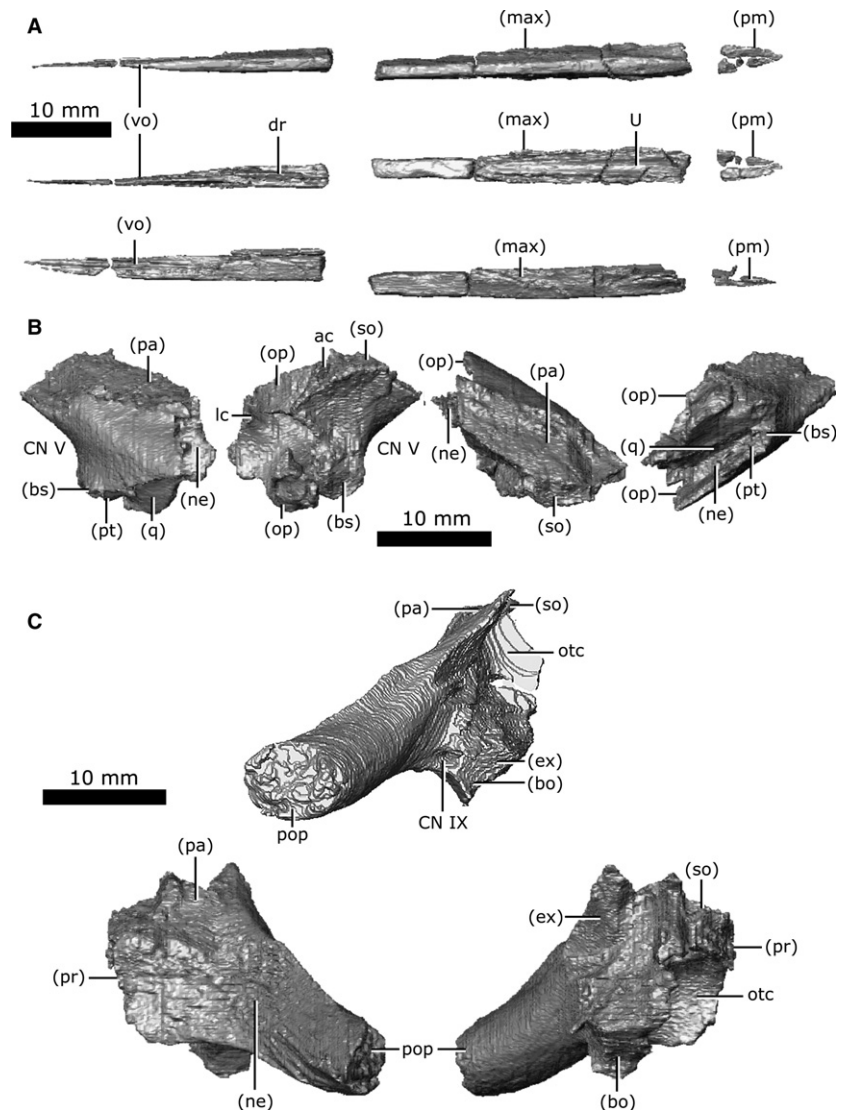


Fig. 16 Isolated internarial, prootic, and opisthotic of *Champsosaurus lindoei* (CMN 8920). (A) internarial in ventral view (top), dorsal view (middle), right lateral view (bottom); (B) left prootic in lateral view (left), medial view (second from left), dorsal view (second from right), lateral view (right); (C) left opisthotic in posterior view (top), lateral view (bottom left), medial view (bottom right).

surface of the parietal. The presence of this cavity is the basal condition in Diapsida and is a product of the lack of ossification in the otic region (Evans, 2008).

Exoccipital

Both exoccipitals are preserved in CMN 8920 and are only slightly fractured (Fig. 17B). The exoccipital is a column-like element when viewed posteriorly that forms the lateral wall of the posterior portion of the brain cavity and the lateral margin of the foramen magnum. It originates anteriorly about level with the crus communis, separating the supraoccipital from the opisthotic, contacting the parietal dorsally, and the brain cavity ventrally. The suture with the opisthotic is internally obscured due to fracturing and partial fusion between these two elements, but the external suture is clearly visible. The exoccipital expands posteroventrally to contact the basioccipital. In posterior view, a flange occurs on the ventral portion of the posterior surface (Fig. 17B; flan), likely to have

articulated with the first cervical vertebra, as reported by Brown (1905). The metotic foramen passes through the exoccipital for the majority of its length, exiting the skull posteriorly between the exoccipital and opisthotic (Fig. 17B; mf). This foramen likely carried the vagus (CN X) and accessory (CN XI) nerves, which usually exit the skull together through the metotic foramen between the opisthotic and exoccipital (Romer, 1956; Bellairs & Kamal, 1981; Rieppel, 1985). The passage of the metotic foramen through the exoccipital seems unusual, but is likely due to the partial fusion of the exoccipital and opisthotic. Posterior to the metotic foramen, two paired canals pass through the exoccipital that likely housed branches of the hypoglossal nerve (Fig. 17B; CN XII), which often exit the skull through the exoccipital (Romer, 1956; Bellairs & Kamal, 1981). The ventral-most canal is narrow (less than 1 mm across) and was not identified by Fox (1968), who described CN XII as exiting as a single root through the exoccipital.

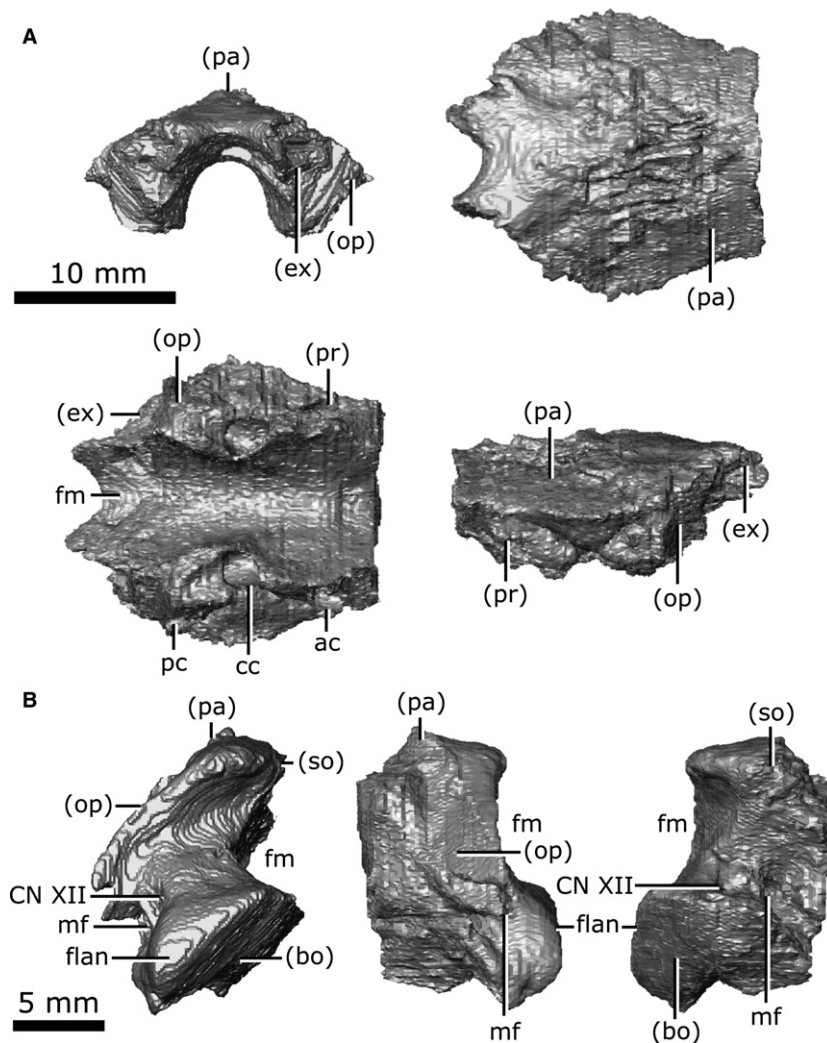


Fig. 17 Isolated supraoccipital and exoccipital of *Champsosaurus lindoei* (CMN 8920). (A) supraoccipital in posterior view (top left), dorsal view (top right), ventral view (bottom left), left lateral view (bottom right); (B) left exoccipital in posterior view (left), lateral view (middle), medial view (right).

Parasphenoid

Although the parasphenoid is technically a dermatocranial ossification, it is included here with the chondrocranial elements due to its frequent fusion with the chondrocranial basisphenoid across Amniota (see Discussion for details). Russell (1956) identified this element as having completely fused with the basisphenoid in *C. natator*, but the CT data show that it is a distinct ossification in *C. lindoei*, and the two elements only show fusion in a small section at the centre of their shared suture. The parasphenoid has undergone slight fragmentation along its length, but otherwise remains undistorted (Fig. 18). This element is triangular when viewed ventrally, but is fractured in CMN 8920, where the posterior tips and a portion in the middle has not been preserved. The ventral surface of the parasphenoid possesses a depression that represents the median pharyngeal recess (Fig. 18; mpr). The parasphenoid originates anteriorly, medial to the quadrate rami of the pterygoids, just anterior to the anterior-most point of the basisphenoid. The canals

for the carotid arteries can be seen on the ventral surface of the parasphenoid where the basisphenoid originates. Anteriorly, the parasphenoid is covered dorsally by the basisphenoid. As the parasphenoid extends posteriorly, it forms the ventral surface of the axially symmetrical basal tubera (Fig. 18; bt), and a prominent dorsal keel forms medial to the otic capsules (Fig. 18; k). The dorsal keel remains prominent until the parasphenoid meets the basioccipital dorsally, where the keel terminates and the bone becomes flat and thin. Fox (1968) described the keel as a low ridge, but the CT data clearly show the keel is prominent. The basal tubera of the parasphenoid extend posterolaterally, but are terminated by breakage. Intact specimens of *C. gigas* (Erickson, 1972) suggest that the parasphenoid would not have continued much farther than that seen in CMN 8920 and would naturally truncate in a smooth rounded projection. The parasphenoid partially forms the posterior floor of the endocranial cavity, as well as the medial rim of the fenestra ovalis.

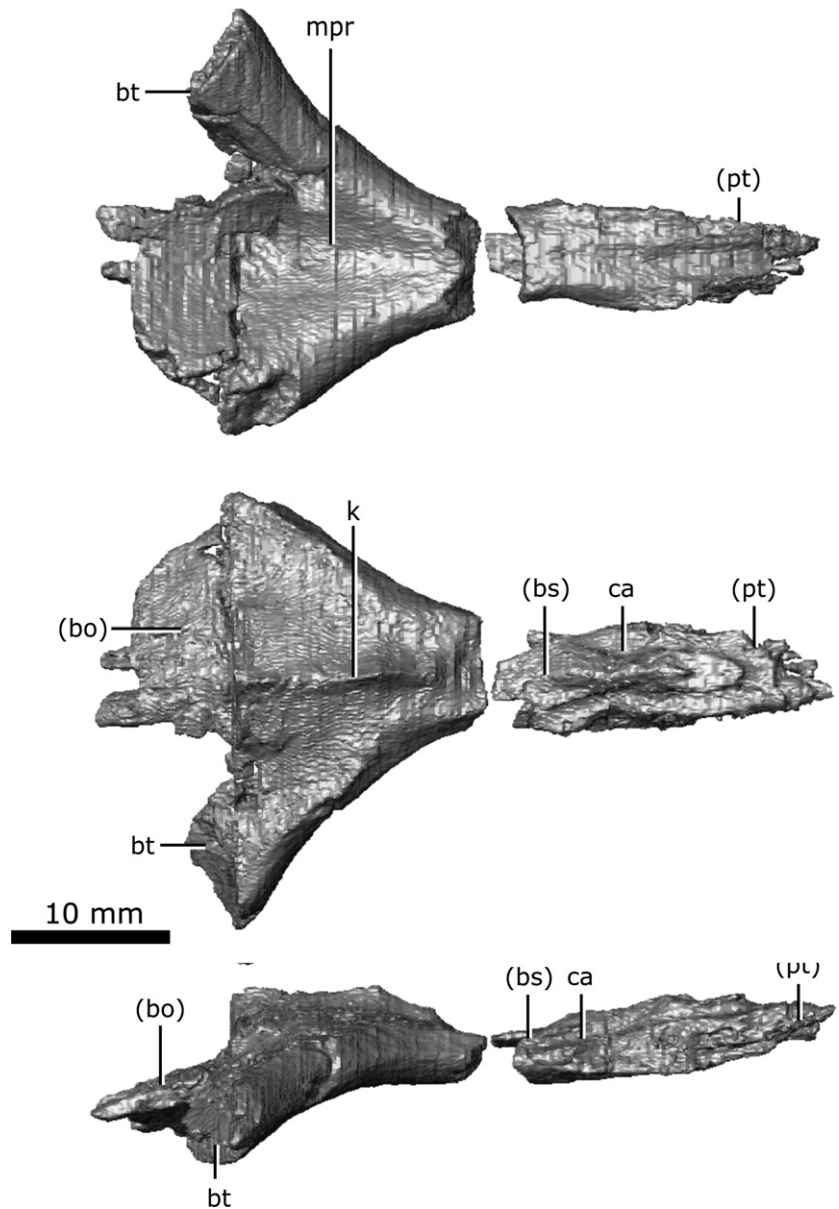


Fig. 18 Isolated parasphenoid of *Champsosaurus lindoei* (CMN 8920) in ventral view (top), dorsal view (middle), right lateral view (bottom).

Basisphenoid

The basisphenoid is well-preserved in CMN 8920 with little fracturing (Fig. 19A). When viewed laterally, the basisphenoid is roughly triangular in outline due to the dorsally expanded clinoid processes. These clinoid processes (Fig. 19A; cp) form a distinct concave-up trough when viewed anteriorly to house the midbrain. The base of this trough forms the posterior margin of the pituitary fossa and the ventral rim of the CN V opening. A long and slender canal that held CN VI extends anteriorly from the ventral surface of the cavity to the lateral wall of the clinoid process. The basisphenoid contacts the parasphenoid ventrally for its entire length, and the quadrate rami of the pterygoids ventrolaterally. Together, the basisphenoid and the pterygoid form a trough lateral to the brain cavity that

housed the lateral head vein. The basisphenoid contacts the prootic laterally and becomes dorsoventrally compressed and flattened. The canals for the internal carotid arteries enter the skull between the pterygoid laterally and parasphenoid medially, and are roofed by the basisphenoid.

Basioccipital

The basioccipital is well-preserved in CMN 8920, with the exception of the basal tubera, which have fractured away at the base (Fig. 19B; bt). The basioccipital is located dorsal to the parasphenoid and forms the posterior-most floor of the endocranial cavity. The occipital condyle is symmetrical, and has a shallow groove situated medially on the dorsal surface, giving it a reniform shape in posterior view (Fig. 19B; oc). As the brain cavity reduces in volume and

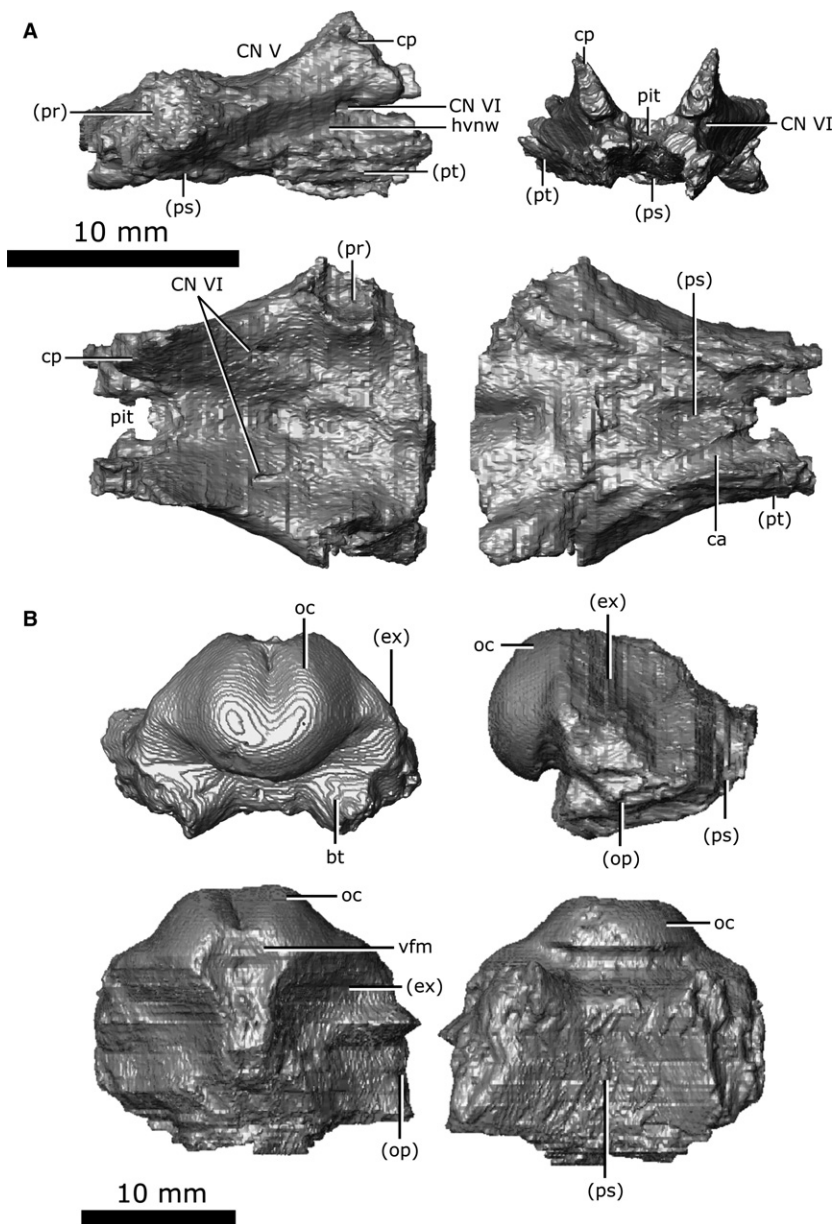


Fig. 19 Isolated basisphenoid and basioccipital of *Champsosaurus lindoei* (CMN 8920). (A) basisphenoid in right lateral view (top left), anterior view (top right), dorsal view (bottom left), ventral view (bottom right); (B) basioccipital in posterior view (top left), right lateral view (top right), dorsal view (bottom left), ventral view (bottom right).

diameter towards the foramen magnum, the exoccipital and the opisthotic contact the basisphenoid laterally, and the parasphenoid terminates, allowing the basisphenoid to be exposed on the ventral surface. Posteriorly, the opisthotics diverge laterally, leaving only a portion of the exoccipital in contact with the basioccipital. The exoccipital and basisphenoid diminish and terminate at the foramen magnum, where the basioccipital forms the occipital condyle.

Discussion

This study provides the first exhaustive description of the skull of a choristodere using micro-CT data, and has allowed the cranial bones of *Champsosaurus* to be imaged and described in three dimensions for the first time. The

data reported in the present study confirm that the neomorphic ossification is distinct, and is not an extension of one of the neighbouring bones. Despite this confirmation, we chose not to give the neomorph a unique name because renaming an element that has been consistently referred to as the 'choristoderan neomorph' for over 50 years would likely cause unnecessary confusion in the literature. The neomorphic ossification has previously been reported in all neochoristoderes (Fox, 1968; Erickson, 1987; Brinkman & Dong, 1993; Ksepka et al. 2005), but the sutures surrounding the bone were often obscured by breakage or matrix. Although the neomorph was interpreted as elongate in these taxa, the presence and morphology of this element was ambiguous. Confirmation of the neomorph as elongate in *Champsosaurus* supports

previous interpretations of an elongate neomorph in all other neochoristoderes.

A recent publication describing a non-neochoristoderan choristodere (henceforth simply non-neochoristodere) from the Upper Jurassic (Oxfordian) of China, *Coeruleodraco jurassicus* (IVPP V 23318; Matsumoto et al. 2019), suggests that the neomorphic bone is present in this taxon; however, the validity of the neomorphic bone was not discussed, nor the wider implications of its presence in *Coeruleodraco*. Our data support the observations of Matsumoto et al. (2019), suggesting that the neomorph is present in all choristoderes more derived than *Coeruleodraco* (i.e. all choristoderes other than *Cteniogenys*; Matsumoto et al. 2019). Evans (1990) inferred the presence of the neomorph in *Cteniogenys* based on facets in the neighbouring bones, a conclusion that is now supported by the presence of this element in other choristoderes. It therefore seems probable that the neomorphic ossification is a synapomorphy of Choristodera, but a thorough description of the element in other non-neochoristoderes is needed to confirm this.

The groove on the lateral surface of the parietal and neomorph is not well understood, but it has been suggested to correlate with the stapedia branch of the carotid artery (Fox, 1968). Given that this groove extends from the opening for CN V to the pterygoquadrate foramen, it may be possible that this groove carried the mandibular branch of the trigeminal nerve (CN V₃), which would have extended ventrally through the pterygoquadrate foramen and entered the jaw.

Lu et al. (1999) described an enlarged pineal system in *Ikechosaurus* that extends dorsally and is roofed by the parietals. The concavity on the ventral surface of the parietals of CMN 8920 suggests that *C. lindoei* also possessed an enlarged pineal system, a feature that may therefore be common to Neochoristodera. Lu et al. (1999) also reported a short and simple series of tubes extending dorsally from the pineal body into the parietal that they interpreted as a remnant of the pineal eye, but no such structures were seen in CMN 8920. This suggests that the pineal eye has been completely lost in *C. lindoei*, and there is no internal evidence to indicate its presence within the cranium.

Lu et al. (1999) identified a small paired gap between the vomer and palatine of *Ikechosaurus* that may have housed the vomeronasal organ; however, no such structure is present in CMN 8920, nor has it been reported in other choristoderes. This leads to the conclusion that *C. lindoei*, and choristoderes more broadly, reduced or lost the vomeronasal organ.

The nasopalatal trough (narial trench of Brown, 1905; narial groove of Russell, 1956; palatonasal trough of Erickson, 1985), unique to choristoderes, is shallow but distinct in CMN 8920. The function of this trough is not well understood, but it may have supported a soft tissue extension of the nasal passage posterior to the choanae (Erickson, 1985).

The nasopalatal trough was once considered to be a synapomorphy of Neochoristodera (Gao & Fox, 1998), but may also be present in some non-neochoristoderes (e.g. *Monjurosuchus*; Gao et al. 2007).

Although the epipterygoid is not preserved in CMN 8920, this element has been reported in other specimens. Fox (1968) reported the epipterygoid in *C. natator* (subsequently identified as *C. lindoei*; Gao & Fox, 1998) as a paired, slender element that projects anterodorsally over the pterygoid from the basisphenoid trough. This element is only reported in a few specimens of *Champsosaurus* (Gao & Fox, 1998), likely due to its gracile shape and fragility.

As is typical for stem-diapsids (Romer, 1956), the ossified chondrocranium does not fully enclose the brain cavity in *C. lindoei*, where the anterior portions of the chondrocranium would remain cartilaginous in life and would also be supplemented anterodorsally by several dermatocranial elements (e.g. parietals and frontals). The parasphenoid and basisphenoid often fuse completely in amniotes to form the parabasisphenoid; however, complete fusion of these elements does not occur in *C. lindoei*. These elements only undergo fusion over a small portion of their shared surface internally, a feature that is evident from the CT data as the suture vanishes internally and the two bones become confluent. A similar condition is seen between the exoccipital and the opisthotic. These elements often fuse completely in diapsids to form the otoccipital, but this is not seen in *C. lindoei*. An external suture between the exoccipital and opisthotic is clearly visible in CMN 8920, other specimens of *C. lindoei*, and other species of *Champsosaurus* (Fox, 1968; Gao & Fox, 1998). Internally, these bones remain separate for the majority of their shared surfaces, only becoming fused for a small portion near the endocranial cavity.

The CT data from CMN 8920 indicate that the paired, ventrally oriented gaps lateral to the parasphenoid enclosed the fenestrae ovals (Fig. 20), supporting Fox's (1968) interpretation. Supporting this conclusion is the fact that there is no other opening to the inner ear at which the stapes could have articulated. Fox (1968) states that these openings commune to the otic capsule laterally, but the CT data show that these openings actually commune to it ventrally. Based on images and illustrations in the literature, these gaps also occur in *Simoedosaurus dakotensis* (SMM P76.10.1; Erickson, 1987) and *Ikechosaurus sunailinae* (IVPP V9611-3; Brinkman & Dong, 1993), suggesting that a ventrally oriented fenestra ovalis is synapomorphic to Neochoristodera. This arrangement cannot be determined at present in non-neochoristoderes because few specimens are preserved with the ventral surface exposed, and those that are tend to be heavily fractured, obscuring the braincase. A ventrally oriented fenestra ovalis is unusual among tetrapods, but it has been reported in other aquatic taxa, such as some plesiosaurs (e.g. *Dolichorhynchops*; Sato et al. 2011), some aistopods (e.g. Phlegethontiidae; Clack & Anderson, 2016; Pardo et al. 2019), and some urodeles (e.g. *Siren*;

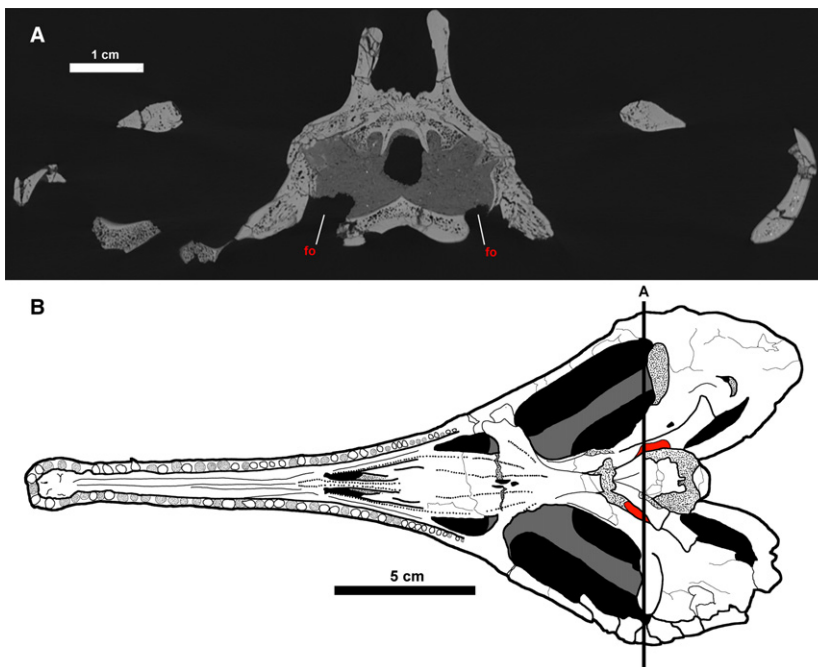


Fig. 20 The fenestrae ovals of *Champsosaurus lindoei*. (A) coronal cross section of the braincase of CMN 8920; (B) ventral view of CMN 8920 with the fenestrae ovals coloured red. Black line labelled 'A' indicates the position of cross section A. Fine stippling indicates fractured surfaces exposing cancellous bone.

Reilly & Altig, 1996). The functional implications of this morphology in *Champsosaurus* will be the subject of future work.

Conservation of the braincase among amniotes and its implications for the choristoderan neomorph ossification

The choristoderan neomorph bone has previously been described as a component of the braincase (Fox, 1968; Brinkman & Dong, 1993; Gao & Fox, 2005; James, 2010), likely due to its external location on the lateral wall of the braincase, but the internal connections of the element remained poorly understood. Now that the existence of the neomorph has been confirmed, and its morphology described, it should be determined whether this element should be properly defined as a braincase bone. As stated in the Introduction, the braincase is defined here as all bones within the chondrocranium, plus the parasphenoid, which often fuses with chondrocranial elements (Atkins & Franz-Odenaal, 2016). Since it has been shown here that the neomorph bone is not fused with any chondrocranial element, in order to classify the neomorph as a braincase bone, it must be determined whether it is chondrocranial in origin. Although the developmental path of a structure in an extinct taxon cannot be absolutely determined (Romer, 1956), possible developmental paths can be hypothesized based on the variation seen in the development of cranial bones in living amniotes. If it is found that the complement of bones in the chondrocranium tends to be conserved, it can be concluded that an element peripheral to this conserved complement is unlikely to be chondrocranial, and

the neomorph bone will therefore not be classified here as a braincase bone.

Based on the condition seen in early reptiles, the ancestral braincase of Amniota is inferred to consist of the supraoccipital, exoccipital, basioccipital, basisphenoid, opisthotic, prootic and parasphenoid (Romer & Parsons, 1977). With the exception of the parasphenoid, these elements form as ossifications of the chondrocranium around the posterior portion of the brain cavity, where the anterior portion remains enclosed by cartilage into maturity (Romer, 1956). Although fusion of chondrocranial elements is well known (e.g. fusion of the exoccipital and opisthotic to form the otoccipital in some archosaurs; Knoll et al. 2012) the development of new ossifications of the chondrocranium is considered exceedingly rare (Cardini & Elton, 2008; Goswami & Polly, 2010; Knoll et al. 2012; Maddin et al. 2012). To illustrate this, ossifications from the braincase in several lineages of amniotes have been tabulated for a broad comparison (Table 2).

Based on the data derived from Table 2, there are apparently three novel bones that originate from the chondrocranium; the laterosphenoid, orbitosphenoid and internarial. In archosaurs, the laterosphenoid forms as an ossification of the anterior chondrocranium (more specifically, from the cartilaginous pila antotica) between the exits for CN III, CN IV and CN V, and ventrally supports the anterior portion of the brain (Evans, 2008; Sobral et al. 2016). The laterosphenoid also occurs in fossil stem turtles and may suggest that turtles are a sister-group to archosaurs (Bhullar & Bever, 2009).

The orbitosphenoid is represented by cartilage in basal amniotes (de Beer, 1937), but can ossify in some lineages of

Table 2 A comparison of braincase bones across Amniota.

	Prootic	Supraoccipital	Opisthotic	Exoccipital	Basioccipital	Basisphenoid	Parasphenoid	Laterosphenoid	Orbitosphenoid	Internarial
<i>Anthracosauria</i>										
<i>Palaeoherpeton</i> sp.	X	X	X	X	X	X	X			
<i>Seymouriamorpha</i>										
<i>Seymouria</i> sp.	X	X	X	X	X	X	X			
Stem-Neodiapsida										
<i>Youngina capensis</i>	X	X	X	X	X	X*	X*			
<i>Neodiapsida incertae sedis</i>										
<i>Champsosaurus lindoei</i>	X	X	X	X	X	X	X			X†
Sauropterygia										
<i>Nothosaurus</i> sp.	X	X	X	X	X	X*	X*			
Pantestudines										
<i>Proganochelys quenstedti</i>	X	X	X	X	X	X*	X*	X		
<i>Meiolania platyceps</i>	X	X	X	X	X	X*	X*			
<i>Pseudemys texana</i>	X	X	X	X	X	X*	X*			
<i>Sternotherus oderatus</i>	X	X	X	X	X	X*	X*			
<i>Archosauria</i>										
<i>Erythrosuchus africanus</i>	X	X	X†	X†	X	X*	X*	X		
<i>Euparkeria capensis</i>	X	X	X	X	X	X*	X*	X	X	
<i>Stenonychosaurus inequalis</i>	X	X	X†	X†	X	X*	X*	X	X	
<i>Spinophorosaurus nigerensis</i>	X	X	X†	X†	X	X*	X*	X	X	
<i>Lesothosaurus diagnosticus</i>	X	X	X	X	X	X*	X*	X	X	
<i>Alligator mississippiensis</i>	X	X	X	X	X	X*	X*	X	X	
Rhynchocephalia										
<i>Sphenodon punctatus</i>	X	X	X	X	X	X*	X*			
Squamata										
<i>Trachylepis laevis</i>	X	X	X†	X†	X	X*	X*		X	
<i>Shinisaurus crocodilurus</i>	X	X	X†	X†	X	X*	X*		X	
<i>Iguana iguana</i>	X	X	X†	X†	X	X*	X*		X	
<i>Diplometopon zarudnyi</i>	X	X	X	X	X	X*	X*	X	X	
<i>Varanus exanthematicus</i>	X	X	X†	X†	X	X*	X*			
<i>Varanus priscus</i>	X	X	X†	X†	X	X*	X*			
<i>Tupinambis nigropunctatus</i>	X	X	X†	X†	X	X*	X*		X	
<i>Pogona vitticeps</i>	X	X	X†	X†	X	X*	X*		X	

Alligator mississippiensis – Rowe et al. (1999); *Diplometopon zarudnyi* – Abo-Eleneen et al. (2017); *Erythrosuchus africanus* – Gower (1997); *Euparkeria capensis* – Gower & Weber (1998); *Iguana iguana* – Lima et al. (2014); *Lesothosaurus diagnosticus* – Sereno (1991); *Meiolania platyceps* – Gaffney (1983); *Nothosaurus* sp. – Rieppel (1994); *Palaeoherpeton (Palaeoogryinus)* of Romer, 1956 – Romer (1956); *Pogona vitticeps* – Ollonen et al. (2018); *Proganochelys quenstedti* – Gaffney (1990); Bhullar & Bever (2009); *Pseudemys texana* – Bever (2009); *Seymouria* – Romer (1956); *Spinophorosaurus nigerensis* – Knoll et al. (2012); *Shinisaurus crocodilurus* – Bever et al. (2005); *Sphenodon punctatus* – Romer (1956); Sobral et al. (2016); *Stenonychosaurus inequalis* – Currie (1985); *Sternotherus oderatus* – Bever (2009); *Trachylepis laevis* – Paluh & Bauer (2017); *Tupinambis nigropunctatus* – Jollie (1960); *Youngina capensis* – Gardner et al. (2010); *Varanus exanthematicus* – Rieppel & Zaher (2000); *Varanus priscus* – Head et al. (2009).

†'X' indicates the bone is present. *Elements have fused to form the parabasiphenoid; †fused to form the otoccipital; ‡may be dermatocranial.

archosaurs, lepidosaurs and mammals (Hernandez-Jaimes et al. 2012; Benoit et al. 2017). When present, this element is found anterior to the laterosphenoid, located between the exits for CN II, CN III and CN IV, and usually forms as an ossification from the pila metoptica (Evans, 2008) and the taenia medialis (de Beer, 1937; Benoit et al. 2017). The ossification of this region of the chondrocranium is highly variable between species and appears to have evolved several times independently. The variability in the ossification of this region may correlate with the distribution of bite force across the chondrocranium (Evans, 2008; Jones et al. 2017).

The internarial element is unique to *Champsosaurus* and is a diagnostic feature of the genus (Gao & Fox, 1998; Matsumoto et al. 2013). The internarial was described as a neomorphic ossification by Russell (1956), Romer (1956) and Erickson (1972), and is possibly derived from the cartilaginous internarial septum (Russell, 1956). The CT data presented here indicate that the internarial possesses a ridge on the dorsal surface that extends into the nasal cavity and may have supported the cartilaginous internarial septum. This evidence could support the previous hypothesis that the internarial is derived from the cartilaginous internarial septum due to their close association to one another in the skull. Alternatively, the internarial bone may have ossified from the dermatocranium, given that the septum does not ossify other than on the palatal surface. At present, there is insufficient evidence to determine whether the internarial is of dermal or chondrocranial origin, but it is tentatively designated here as a chondrocranial ossification due to its previous description as an ossification from the internarial septum (Russell, 1956).

What is clear from the comparison of braincase bones across Amniota (Table 2) is that, although the anterior chondrocranium shows some variation in ossification between taxa, there are neither new ossifications nor re-ossifications in the posterior region across Amniota. The posterior braincase shows an overall trend towards reduction in the number of discrete elements through fusion, i.e. the basisphenoid and parasphenoid often fuse to form the parabasisphenoid, and the exoccipital and the opisthotic often fuse to form the otoccipital (Knoll et al. 2012). This trend in the reduction of discrete elements is also reported in Lissamphibia (Atkins et al. 2019), suggesting that braincase simplification may be common in tetrapods. Therefore, the appearance of a novel ossification in the posterior chondrocranium of chorisotoderes is highly unlikely. Additionally, the neomorph does not fuse with chondrocranial elements, as does the dermatocranial parasphenoid, and so it fails to meet the parameters of inclusion to the chondrocranium that are applied to the parasphenoid in this study. Although the exact developmental path of a structure cannot be determined in extinct taxa (Romer, 1956), the chorisotoderan neomorphic bone is probably not chondrocranial in origin. Based on these facts, we posit that the chorisotoderan neomorphic bone should not be considered as a

braincase element, but instead as an element that occurs lateral, but attached, to the braincase. Further to this suggestion, even when using a less conservative definition of a braincase bone (the third definition: any bone that contacts the brain cavity), the neomorphic bone still fails to meet this definition as it is clearly separated from the endocranial cavity by the underlying prootic and opisthotic (Fig. 21).

There are two other possibilities regarding the origin of the neomorph: it is splanchnocranial and developed from the embryonic gill arches, or it is dermatocranial and developed as an intramembranous ossification. It seems highly unlikely that the neomorph developed from the splanchnocranium, as a novel development from the embryonic gill arches has not occurred since the evolution of ossified jaws (e.g. the articular element of osteichthians; DeLaurier, 2018). Additionally, it is impossible for the neomorph to have developed as a modification of a pre-existing splanchnocranial element in the jaw (as seen in the inner ear bones of mammals) as all the typical reptilian jaw bones are found in the *Champsosaurus* mandible (Brown, 1905). The stapes is the only undescribed splanchnocranial element in chorisotoderes and may be homologous with the neomorph. The possible homology of the neomorph and stapes is supported by: (1) the ancestral role of the stapes as a structural element in the diapsid skull (and in amniotes and tetrapods more generally; Carroll, 1980; Carroll, 1982; Gardner et al. 2010); (2) the medial articulation of the neomorph with the prootic and opisthotic of the otic capsule; (3) the lateral articulation of the neomorph with the quadrate; and (4) the presence of a foramen (the pterygoquadrate foramen) penetrating the neomorph that may be homologous with the stapedia foramen. Matsumoto et al. (2019) found that the early non-neochorisotodere, *Coeruleodraco*, may possess both the stapes and the neomorphic bone, suggesting that these elements are not homologous; however, they acknowledged that the identification of the stapes was hindered by low scanning resolution, and is therefore inconclusive. The data reported in the present study suggest that a more precise description of the putative stapes in *Coeruleodraco* is needed to comment on the presence and morphology of the bone in that taxon.

The only other possible origin of the neomorphic bone is as a novel ossification from the dermatocranium. These bones often form through intramembranous ossification, where the bones arise directly from the cranial dermis, and lack cartilaginous precursors (Romer & Parsons, 1977). Although cranial anatomy shows a trend towards fewer discrete elements over time (Sidor, 2001; Table 2), the known instances of neomorphic ossifications (e.g. the palpebral found in some lacertoids, cordyloids, scincoids and anguimorphs, the supraorbital found in pythonid snakes, and the parafrontal of some gekkos; Estes et al. 1988; Conrad, 2008; Daza & Bauer, 2010) have developed from the dermatocranium, making it a good candidate for the origin of the chorisotoderan neomorph.

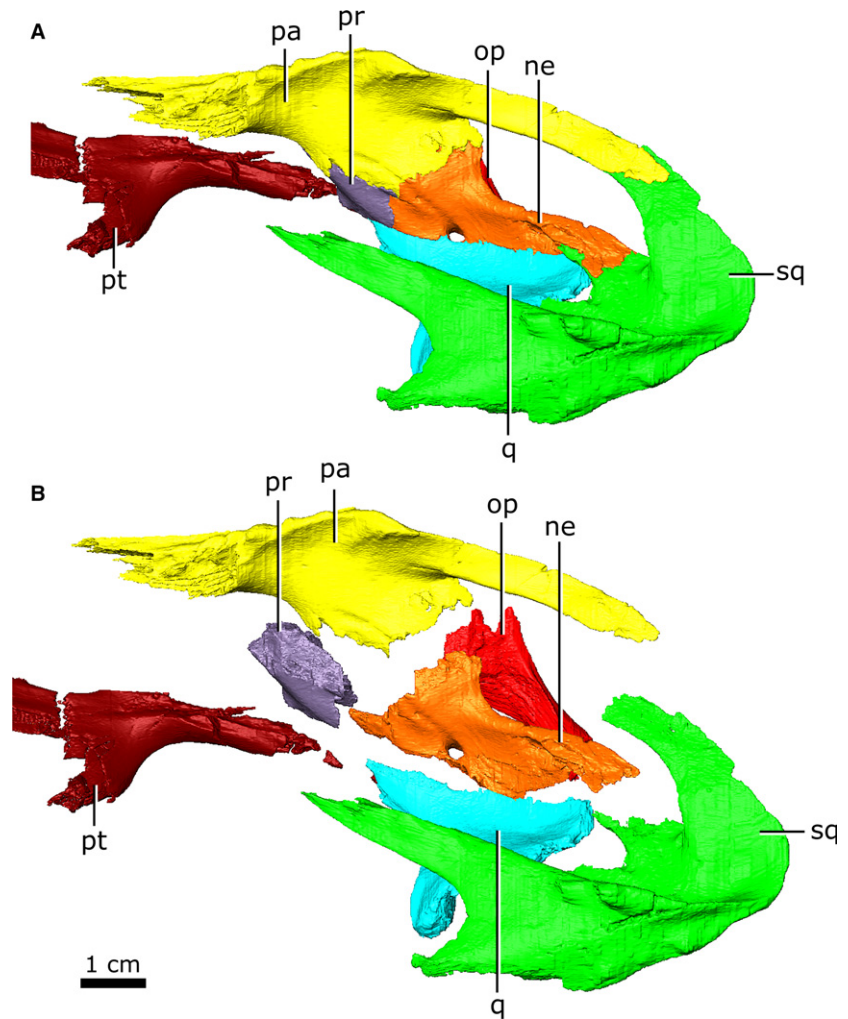


Fig. 21 Left neomorphic bone and adjoining bones of *Champsosaurus lindoei* (CMN 8920) in left dorsolateral view with the elements (A) articulated, and (B) exploded.

What remains elusive is how neomorphic ossifications are instigated in the developing cranium. Although there are many possible developmental origins of dermatocranial neomorphic ossifications, a common mechanism is through the subdivision of pre-existing elements (Sidor, 2001). Subdivision can occur through the incomplete fusion of multiple ossification sites of a single element (Romer, 1956), and is known to produce the jointed premaxilla of bolyerine snakes (Frazzetta, 1970), and the neomorphic echidna pterygoid (de Beer, 1937) that forms three bones instead of two. It is most probable that the choristoderan neomorphic bone developed via the subdivision of a pre-existing element, as this mechanism is most prominent in the formation of dermatocranial neomorphic bones in amniotes. If this is true, it means the neomorph developed from one of the surrounding bones in the skull, but determining conclusively which bone it could have developed from is difficult. The simplest way to determine possible origins of the neomorph, other than finding embryonic choristoderans with the neomorphic bone preserved, would be to observe the bones in

contact with this element and determine the likelihood of the neomorph originating from these elements.

In CMN 8920, the neomorphic bone is in contact with the prootic, opisthotic, pterygoid, squamosal, quadrate and parietal (Fig. 21). In the early choristodere *Coeruleodraco*, the neomorph appears to only contact the parietal, opisthotic and a small portion of the squamosal (Matsumoto et al. 2019). Although the neomorphic bone is more accurately described here in *Champsosaurus*, the morphology of the neomorph in the more basal *Coeruleodraco* (Fig. 22) is more likely to resemble the ancestral condition, and can therefore provide more accurate information regarding its origin.

In *Coeruleodraco*, the neomorph appears to only briefly contact the squamosal at its posterior-most extent (Fig. 22). This suture is very short, and it is therefore unlikely that the neomorph developed from this element. The neomorph shares extensive sutures with both the opisthotic and parietal, but, based on the rarity of neomorphic bones developing from chondrocranial elements (Table 2) and the abundance of neomorphic bones developing from the

dermatocranium (Estes et al. 1988; Conrad, 2008; Daza & Bauer, 2010), it might be concluded that the neomorphic bone developed from the parietal, although this is entirely speculative at present.

Functionality of the choristoderan neomorphic ossification

The functionality of the neomorphic bone in the early choristodere *Coeruleodraco* is hard to determine, given that this element is interpreted as quite small and does not appear to be structural. Prior to the discovery of this genus, the neomorph has always been found in conjunction with the pterygoquadrate foramen (pterygoid foramen of Matsumoto et al. 2019), and it is therefore possible that those two structures were related. The discovery of *Coeruleodraco* refutes this, where the neomorphic bone appears to occur in the absence of the pterygoquadrate foramen, suggesting that this foramen may be a synapomorphy of Neochoristodera. This conclusion is supported by the apparent absence of the pterygoquadrate foramen in all known non-neochoristoderes, but these specimens were too damaged to definitively determine if the pterygoquadrate foramen and neomorphic bone were present (Evans, 1990; Gao & Fox, 2005; Gao & Ksepka, 2008).

Fox (1968) suggested that the neomorph developed to strengthen the connection between the braincase and the pterygoquadrate region, but the small size of the neomorph reported in *Coeruleodraco* (Matsumoto et al. 2019) makes this unlikely. As such, it is possible that the neomorphic ossification did not develop due to some driving selection pressure, but developed randomly and became fixed in the population because it had no deleterious effects. Such traits could develop by chance through genetic drift or as an evolutionary spandrel (Lande, 1976; Gould & Lewontin, 1979; Dieckmann & Doebeli, 1999).

Regardless of its origin, once instigated, the morphology and function of this element was free to change. Given the size and location of the neomorph at the base of the temporal arches in *Champsosaurus*, a possible derived function of this element in neochoristoderes is to strengthen the

connection between the large temporal arches and the braincase and palatal region (Fox, 1968). A potential advantage to enlarging the neomorph is the expansion of the surrounding sutures. The primary role of sutures in the mature skull is for stress transfer and dampening (Pritchard et al. 1956; Curtis et al. 2013), where the sutures reduce the stress gradient between bones and distribute the bite force evenly across the skull (Mao, 2002; Kopher & Mao, 2003; Curtis et al. 2013). Increasing the length of sutures at the base of the temporal arches could be beneficial, as they would help absorb and distribute the mechanical stress from biting.

James (2010) described the feeding mechanics of *Champsosaurus*, and he calculated that these animals could generate bite forces that are equal to and potentially greater than those of similarly sized modern crocodylians. Alligators are known to increase the width of their cranial sutures through ontogeny to better absorb the stress on the skull when biting (Erickson et al. 2003; Bailleul et al. 2016). However, if a suture becomes too wide it can allow the skull to flex and become kinetic, which dampens bite force (Iordansky, 1990). As such, a neomorphic ossification in *Champsosaurus* could provide an optimal state, increasing the number of sutures to better distribute stress while maintaining the strength and rigidity of the skull.

A second possible function of the neomorph in *Champsosaurus* is to increase the size of the attachment sites for the jaw adductors; however, this is dubious because the neomorph was unlikely to have played a large role in supporting jaw muscles (James, 2010), and it is difficult to explain how the jaw muscles could not be supported by the pre-existing bones of the skull. It is also possible that the enlargement of the neomorphic ossification over evolutionary time is simply due to the expansion of the temporal region in neochoristoderes. The other bones of the temporal region (i.e. parietal, squamosal, postorbital, quadratojugal) are all elongated in neochoristoderes when compared to non-neochoristoderes, and the neomorphic bone could therefore have simply been modified in congruence with the other elements in the expanded temporal region.

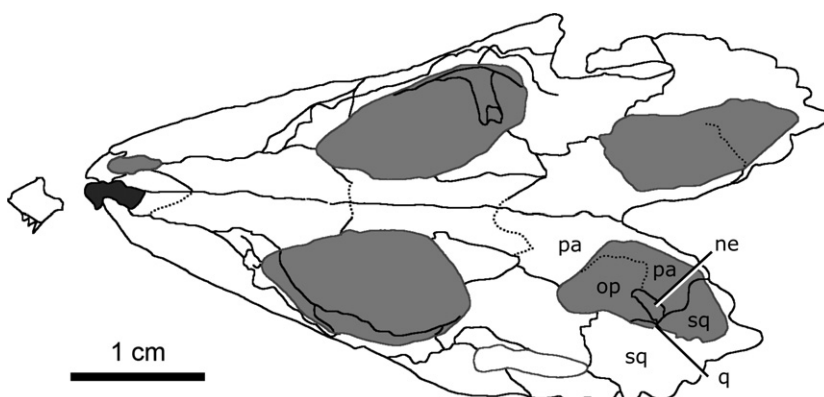


Fig. 22 Line drawing of the skull of *Coeruleodraco jurassicus* (IVPP V 23318) in dorsal view. Modified from Matsumoto et al. (2019).

Conclusions

The present study describes the cranial bones of *C. lindoei* in 3D using CT scanning. The data reveal that the fenestra ovalis of *C. lindoei* is located ventrally on the skull, an unusual feature that may be synapomorphic to Neochoristodera. *Champsosaurus lindoei* was also found to have a large pineal body, like the previously reconstructed *Ikechosaurus* (Lu et al. 1999), but lacked all evidence for a pineal eye and the vomeronasal organ. These data also allowed the confirmation of the neomorphic element, and revealed the nature of its morphology and relationship to other cranial bones.

We provided the first review of the variation seen in amniote chondrocranial ossifications, which illustrates how this region of the skull tends to be evolutionarily conserved, showing a trend towards simplicity over time. As such, it is concluded that the neomorphic bone is unlikely to have developed from the chondrocranium and therefore should not be described as a braincase bone. The stapes is a pre-existing cranial element that may be homologous with the neomorphic bone, and a more precise description of the putative stapes in *Coeruleodraco* is needed to comment on the presence of the bone in that taxon. If the neomorph is not homologous with the stapes, the most likely developmental membership of the neomorphic bone is as a component of the dermatocranium. The exact developmental mechanism for the origin of the neomorph cannot be determined conclusively, but it is most probable that it developed through the incomplete fusion of ossification centres from a pre-existing cranial bone, possibly the parietal. Given the relatively small size of the neomorph in *Coeruleodraco*, it may not have had a structural role in the skull of early choristoderes and arose through non-adaptive means. In the more derived *Champsosaurus*, the additional sutures surrounding the neomorph may have provided greater stress absorption during biting while maintaining rigidity of the skull; however, it is also probable that the neomorph elongated following the expansion of the temporal region in neochoristoderes.

Acknowledgements

We would like to thank the CMN for providing access to CMN 8920 for study, and the UTCT for scanning CMN 8920. We thank Michael Ryan, Emily Standen, and two anonymous reviewers for their useful comments and improvements to the manuscript. We would also like to thank Jason Anderson and Tetsuto Miyashita for helpful discussions. Funding for this project was provided by NSERC Discovery Grants awarded to J.C.M., H.C.M. and D.C.E.

Data Availability Statement

The CT data generated from this study are available online via MorphoSource (https://www.morphosource.org/Detail/MediaDetail/Show/media_id/46683).

References

- Abo-Eleneen RE, Othman SI, Al-Harbi HM, et al. (2017) Anatomical study of the skull of amphisbaenian *Diplometopon zarudnyi* (Squamata, Amphisbaenia). *Saudi J Biol Sci* **1**, 1–11.
- Atkins JB, Franz-Odenaal TA (2016) The evolutionary and morphological history of the parasphenoid bone in vertebrates. *Acta Zool* **97**, 255–263.
- Atkins JB, Reisz R, Maddin HC (2019) Braincase simplification and the origin of lissamphibians. *PLoS ONE* **14**, e0213694.
- Bailleul AM, Scannella JB, Horner JR, et al. (2016) Fusion patterns in the skulls of modern archosaurs reveal that sutures are ambiguous maturity indicators for the Dinosauria. *PLoS ONE* **11**, 1–26.
- de Beer G (1937) *The Development of the Vertebrate Skull*. Toronto: Oxford University Press.
- Bellairs A, Kamal AM (1981) The chondrocranium and the development of the skull in recent reptiles. In: *Biology of the Reptilia Morphology F*, Vol. **11**. (eds Gans C, Parsons TS), pp. 1–283. New York: Academic Press.
- Benoit J, Jasinowski SC, Fernandez V, et al. (2017) The mystery of a missing bone: revealing the orbitosphenoid in basal *Epicynodontia* (Cynodontia, Therapsida) through computed tomography. *Sci Nature* **104**(66), 1–6.
- Bever GS (2009) The postnatal skull of the extant North American turtle *Pseudemys texana* (Cryptodira: Emydidae), with comments on the study of discrete intraspecific variation. *J Morphol* **270**, 97–128.
- Bever GS, Bell JC, Maisano JA (2005) The ossified braincase and cephalic osteoderms on *Shinisaurus crocodilurus* (Squamata, Shinisauridae). *Palaeontol Electron* **8**(1), 1–36.
- Bhullar BAS, Bever GS (2009) An archosaur-like laterosphenoid in early turtles (Reptilia: Pantestudines). *Breviora* **518**, 1–11.
- Brinkman DB, Dong ZM (1993) New material of *Ikechosaurus sunailinae* (Reptilia: Choristodira) from the Early Cretaceous Laohongdong Formation, Ordos Basin, Inner Mongolia, and the interrelationships of the genus. *Can J Earth Sci* **30**, 2153–2162.
- Brown B (1905) The osteology of *Champsosaurus* Cope. *Am Mus Nat Hist Mem* **9**, 1–26.
- Cardini A, Elton S (2008) Does the skull carry a phylogenetic signal? Evolution and modularity in the guenons. *Biol J Lin Soc* **93**, 813–834.
- Carroll RL (1980) The hyomandibular as a supporting element in the skull of primitive tetrapods. In: *The Terrestrial Environment and the Origin of Land Vertebrates* (ed Panchen AL), pp. 293–317. London: Academic.
- Carroll RL (1982) Early evolution of reptiles. *Annu Rev Ecol Syst* **13**(1), 87–109.
- Clack JA, Anderson JS (2016) Early tetrapods. In: *Evolution of the vertebrate ear: evidence from the fossil record* (eds Clack JA, Fay RR, Popper AN), pp. 71–105. New York: Springer.
- Conrad JL (2008) Phylogeny and systematics of Squamata (Reptilia) based on morphology. *Bull Am Mus Nat Hist* **310**, 1–182.
- Currie PJ (1985) Cranial anatomy of *Stenonychosaurus inequalis* (Saurischia, Theropoda) and its bearing on the origin of birds. *Can J Earth Sci* **22**, 1643–1658.
- Curtis N, Jones MEH, Evans SE, et al. (2013) Cranial sutures work collectively to distribute strain throughout the reptile skull. *R Soc Publish* **10**, 1–9.
- Daza JD, Bauer AM (2010) The circumorbital bones of the Gekokota (Reptilia: Squamata). *Anat Rec* **293**, 402–413.

- DeLaurier A** (2018) Evolution and development of the fish jaw skeleton. *Wiley Interdiscip Rev Dev Biol* **8**(2), e337.
- Dieckmann U, Doebeli M** (1999) On the origin of species by sympatric speciation. *Nature* **400**, 354–357.
- Erickson BR** (1972) *The lepidosaurian reptile Champsosaurus* in North America, Vol. 1, pp. 1–91, Saint Paul, MN: Science Museum of Minnesota, Monograph (Paleontology).
- Erickson BR** (1985) Aspects of some anatomical structures of *Champsosaurus* (Reptilia:Eosuchia). *J Vertebr Paleontol* **5**(2), 111–127.
- Erickson BR** (1987) *Simoedosaurus dakotensis*, new species, a diapsid reptile (Archosauromorpha; Choristodera) from the Paleogene of North America. *J Vertebr Paleontol* **7**(3), 237–251.
- Erickson GM, Lappin AK, Vliet KA** (2003) The ontogeny of bite-force performance in American alligator (*Alligator mississippiensis*). *J Zool* **260**, 317–327.
- Estes R, de Queiroz K, Gauthier J** (1988) Phylogenetic relationships within Squamata. In: *Phylogenetic relationships of the lizard families* (eds. Estes R, Pregill G), pp. 119–281. Stanford, CA: Stanford University Press.
- Evans SE** (1990) The skull of *Cteniogenys* (Reptilia: Archosauromorpha) from the middle Jurassic of Oxfordshire. *Zool J Linn Soc* **99**, 205–237.
- Evans SE** (2008) The skull of lizards and tuatara. In: *Biology of the Reptilia, Vol. 20, Morphology H: The skull of Lepidosauria*, (eds Gans C, Gaunt AS, Adler K), pp. 1–347, New York: Society for the Study of Amphibians and Reptiles.
- Evans SE, Klembara J** (2005) A choristoderan reptile (Reptilia: Diapsida) from the Lower Miocene of northwest Bohemia (Czech Republic). *J Vertebr Paleontol* **25**(1), 171–184.
- Fox RC** (1968) Studies of the Late Cretaceous vertebrates: I. The braincase of *Champsosaurus* Cope (Reptilia: Eosuchia). *Copeia* **1**, 100–109.
- Frazzetta TH** (1970) From hopeful monsters to bolyerine snakes? *Am Nat* **104**, 55–72.
- Gaffney ES** (1983) The cranial morphology of the extinct horned turtle *Meiolania platyceps* from the Pleistocene of Lord Howe Island, Australia. *Bull Am Mus Nat Hist* **175**(4), 1–124.
- Gaffney ES** (1990) The comparative osteology of the Triassic turtle *Proganochelys*. *Bull Am Mus Nat Hist* **194**, 1–263.
- Gao K, Fox RC** (1998) New choristoderes (Reptilia: Diapsida) from the Upper Cretaceous and Palaeocene, Alberta and Saskatchewan, Canada, and phylogenetic relationships of Choristodera. *Zool J Linn Soc* **124**, 303–353.
- Gao K, Fox RC** (2005) A new choristodere (Reptilia: Diapsida) from the Lower Cretaceous of western Liaoning Province, China, and phylogenetic relationships of Monjurosuchidae. *Zool J Linn Soc* **145**, 427–444.
- Gao K, Ksepka D** (2008) Osteology and taxonomic revision of *Hyphalosaurus* (Diapsida: Choristodera) from the Lower Cretaceous of Liaoning, China. *J Anat* **212**, 747–768.
- Gao K, Ksepka D, Lianhai H, et al.** (2007) Cranial morphology of an Early Cretaceous Monjurosuchid (Reptilia: Diapsida) from Liaoning Province of China and evolution of the choristoderan palate. *Hist Biol* **19**(3), 215–224.
- Gardner NM, Holliday CM, O’Keefe FR** (2010) The braincase of *Youngina capensis* (Reptilia, Diapsida): New insights from high-resolution CT scanning of the holotype. *Palaeontol Electron* **13**, 1–16.
- Goswami A, Polly PD** (2010) The influence of character correlations on phylogenetic analysis: a case study of the carnivoran skull. In: *Carnivoran Evolution: New Views on Phylogeny, Form and Function* (eds. Goswami A, Friscia A), pp. 141–164. Cambridge: Cambridge University Press.
- Goold SJ, Lewontin RC** (1979) The spandrels of San Marco and the Panglossian paradigm: a critique of the adaptationist programme. *Proc R Soc Lond B* **205**, 581–598.
- Gower DJ** (1997) The braincase of the early archosaurian reptile *Erythrosuchus africanus*. *J Zool* **242**, 557–576.
- Gower DJ, Weber E** (1998) The braincase of *Euparkeria*, and the evolutionary relationships of birds and crocodilians. *Biol Rev* **73**, 367–411.
- Head JJ, Barrett PM, Rayfield EJ** (2009) Neurocranial osteology and systematic relationships of *Varanus (Megalania) prisca* Owen, 1859 (Squamata: Varanidae). *Zool J Linn Soc* **155**(2), 455–457.
- Hernandez-Jaimes C, Jerez A, Ramirez-Pinilla MP** (2012) Embryonic development of the skull of the Andean lizard *PtychoGLOSSUS bicolor* (Squamata, Gymnophthalmidae). *J Anat* **221**, 285–302.
- Hopson JA, Rougier GW** (1993) Braincase structure in the oldest known skull of a therian mammal: Implications for mammalian systematics and cranial evolution. *Am J Sci* **293**, 268–299.
- Iordansky NN** (1990) Evolution of cranial kinesis in lower tetrapods. *Netherlands J Zool* **40**, 32–54.
- James MSB** (2010) The jaw adductor muscles in *Champsosaurus* and their implications for feeding mechanics. Unpublished M.Sc. Thesis, University of Alberta.
- Jollie MT** (1960) The head skeleton of the lizard. *Acta Zool* **1**–64.
- Jones MEH, Groning F, Dute H, et al.** (2017) The biomechanical role of the chondrocranium and sutures in a lizard cranium. *R Soc Publish* **14**, 1–13.
- Knoll F, Witmer LM, Ortega F, et al.** (2012) The braincase of the basal sauropod dinosaur *Spinophorosaurus* and 3D reconstructions of the cranial endocast and inner ear. *PLoS ONE* **7**(1), 1–12.
- Kopher RA, Mao JJ** (2003) Suture growth modulated by the oscillatory component of micromechanical strain. *J Bone Miner Res* **18**(3), 521–528.
- Ksepka DT, Gao K, Norell MA** (2005) A new choristodere from the Cretaceous of Mongolia. *Am Mus Novit* **3468**(22), 1–22.
- Lande R** (1976) Natural selection and random genetic drift in phenotypic evolution. *Evolution* **30**, 314–334.
- Lima FC, Pereira KF, Abe AS, et al.** (2014) Osteologia do neurocrânio de *Iguana iguana iguana* (Squamata: Iguanidae). *Pesquisa Vet Bras* **34**(1), 69–73.
- Lu J, Zhu Q, Cheng X, et al.** (1999) Computed tomography (CT) of nasal cavity of *Ikechosaurus sunailinae* (Reptilia: Choristodera). *Chin Sci Bull* **44**(24), 2277–2281.
- Maddin HC, Russell AP, Anderson JS** (2012) Phylogenetic implications of the morphology of the braincase of caecilian amphibians (Gymnophiona). *Zool J Linn Soc* **166**, 160–201.
- Mao JJ** (2002) Mechanobiology of craniofacial sutures. *J Dent Res* **81**(12), 810–816.
- Matsumoto R, Evans SE** (2010) Choristoderes and the freshwater assemblages of Laurasia. *J Iberian Geol* **36**(2), 253–274.
- Matsumoto R, Evans SE** (2016) Morphology and function of the palatal dentition in Choristodera. *J Anat* **228**, 414–429.
- Matsumoto R, Evans SE, Manabe M** (2007) The choristoderan reptile *Monjurosuchus* from the Early Cretaceous of Japan. *Acta Palaeontol Pol* **52**(2), 329–350.
- Matsumoto R, Buffetaut E, Escuille F, et al.** (2013) New material of the choristodere *Lazarussuchus* (Diapsida, Choristodera)

- from the Paleocene of France. *J Vertebr Paleontol* **33**(2), 319–339.
- Matsumoto R, Dong L, Wang Y, et al.** (2019) The first record of a nearly complete choristodere (Reptilia: Diapsida) from the Upper Jurassic of Hebei Province, People's Republic of China. *J Syst Paleontol* **17**, 1031–1048.
- Ollonen J, Da Silva FO, Mahlow K, et al.** (2018) Skull development, ossification pattern, and adult shape in the emerging lizard model organism *Pogona vitticeps*: A comparative analysis with other squamates. *Front Physiol* **9**, 1–26.
- Paluh DJ, Bauer AM** (2017) Comparative skull anatomy of terrestrial and crevice-dwelling *Trachylepis* skinks (Squamata: Scincidae) with a survey of resources in scincid cranial osteology. *PLoS ONE* **12**(9), 1–34.
- Pardo JD, Holmes R, Anderson JS** (2019) An enigmatic braincase from Five Points, Ohio (Westphalian D) further supports a stem tetrapod position for aistopods. *Earth Environ Sci Trans R Soc Edinb* **109**, 255–264.
- Parks WA** (1933) New species of *Champsosaurus* from the Belly River Formation of Alberta, Canada. *Trans R Soc Canada* **27**(4), 121–143.
- Porto A, de Oliveira FB, Shirai LT, et al.** (2009) The evolution of modularity in the mammalian skull I: Morphological integration patterns and magnitudes. *Evol Biol* **36**, 118–135.
- Pritchard JJ, Scott JH, Girgis FG** (1956) The structure and development of cranial and facial sutures. *J Anat* **90**, 73–86.
- Reilly SM, Altig R** (1996) Cranial ontogeny in *Siren intermedia* (Caudata: Sirenidae): Paedomorphic, metamorphic, and novel patterns of heterochrony. *Copeia* **1996**(1), 29–41.
- Rieppel O** (1985) The recessus scalae tympani and its bearing on the classification of reptiles. *J Herpetol* **19**, 373–384.
- Rieppel O** (1994) The braincases of *Simosaurus* and *Nothosaurus*: Monophyly of the Nothosauridae (Reptilia: Sauropterygia). *J Vertebr Paleontol* **14**(1), 9–23.
- Rieppel O, Zaher H** (2000) The braincases of mosasaurs the relationships of snakes. *Zool J Linn Soc* **129**, 489–514.
- Romer AS** (1956) *Osteology of the Reptiles*. Chicago: The University of Chicago Press.
- Romer AS, Parsons TS** (1977) *The Vertebrate Body*. 5th edn. Toronto: W.B. Saunders Company.
- Rowe T, Brochu CA, Colbert M, et al.** (1999) Alligator: digital atlas of the skull. *Soc Vertebr Paleontol Memoir* **6**, 1–8.
- Russell LS** (1956) The Cretaceous reptile *Champsosaurus natator* parks. *Bull Natl Mus Canada* **145**, 1–51.
- Sato T, Wu XC, Tirabasso A, et al.** (2011) Braincase of a polycotyloid plesiosaur (Reptilia: Sauropterygia) from the Upper Cretaceous of Manitoba, Canada. *J Vertebr Paleontol* **31**(2), 313–329.
- Sereno PC** (1991) *Lesothosaurus*, "fabrosaurids," and the early evolution of Ornithischia. *J Vertebr Paleontol* **11**(2), 168–197.
- Sidor CA** (2001) Simplification as a trend in synapsid cranial evolution. *Evolution* **55**(7), 1419–1442.
- Sobral G, Sookias RB, Bhullar BAS, et al.** (2016) New information on the braincase and inner ear of *Euparkeria capensis* Broom: implications for diapsid and archosaur evolution. *R Soc Open Sci* **3**, 1–41.
- Specht M, Lebrun R, Zollikofer CPE** (2007) Visualizing shape transformation between chimpanzee and human braincases. *Vis Comput* **23**, 743–751.
- Witmer LM, Ridgely RC** (2009) New insights into the brain, braincase, and ear region of tyrannosaurs (Dinosauria, Theropoda), with implications for sensory organization and behavior. *The Anatomical Record* **292**, 1266–1296.